Characterization and Modelling of a faulted oil and gas field (Syria)

Diana Marcela Valverde Niño

Master of Science Thesis

Department of Earth Science
University of Bergen

June 2013

ABSTRACT

The FC is a faulted oil and gas field located onshore, in the southeast of Syria along the Euphrates Graben. In the 2011, a static reservoir model was built by students of IFP School. The same database used in the 2011 model was using in the 2013 model (seismic data, well data, production information). Refinements and new interpretation were necessary in order to simplify the 2011 model and to prepare a proper case study dedicated to education.

The 2013 model included structural, sedimentological and stratigraphical models, definition of facies and distribution of petrophysical properties to get a more realistic geological case. The model is likely more accurate because of the certainty of the data interpreted about thickness of the Lower Rutbah and Mulussa F clastic reservoirs, the structural framework, the environment of deposition based on core data, the correlation of the main maximum flooding surface and the property distribution in the reservoirs. The compartmentalization in the FC field is created for the normal faulting produced during the Upper Cretaceous.

The main uncertainties are related to interpretation of the main reservoir due to the low resolution of the seismic information, depth-time conversion due to the only VSP information in one well over an area of 180km^2.and variation in the thickness and in the areal extension of the reservoir.

The 2013 model could be improved including a new seismic cube and more data from new wells.

ACKNOWLEDGEMENTS

I would firstly like to thank my primary supervisors, Olivier Lerat for his dedicated support throughout the course of the project. He has provided endless encouragement and advice. Also I would like to thank my second supervisor, Prof. Ritske Huismans. In addition, I would also like to thank Vrije University of Amsterdam and University of Bergen to all the knowledge and support during the Master.

I also express my most sincere gratitude to my family in special to my mother, and Maikol for giving me the confidence to study the MSc and believe in my academic abilities.

I would also like to thank Colombia and the support given by Colfuturo which believe in young people to development the Country. To Holland, Norway and France for hosting me this period. I have learnt a substantial amount these years and it has encouraged me to think about further research here.

I would also like to acknowledge and thank my friends especially to Lucila who always give her support for each difficult moment that I had. We have all worked hard and supported each other these years and without them would have found things far more difficult. Thanks guys.

Finally I must thank IFP School for providing me with the data for both an exciting, and challenging project. I feel privileged to have worked with such data.

TABLE OF CONTENT

LIST OF FIGURES AND TABLES

1. INTRODUCTION

The FC is a faulted oil and gas field located onshore, in the southeast of Syria along the Euphrates Graben. It was discovered in the late 1980s and started producing in 1991. (GEO ExPro May 2006). Figure 1.1.

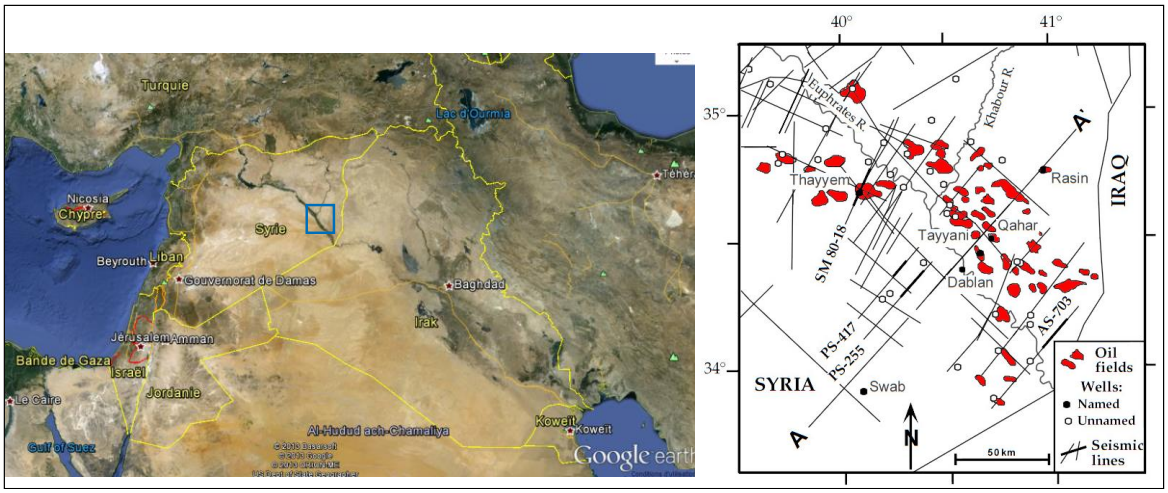

Figure 1.1: Location map of the study area - FC field.

A static reservoir model of the FC field was constructed in 2011 in the context of the European Association of Geosciences & Engineers competition: The Field Challenge. Six students from IFP School were involved in this project, which lasted two months.

The main objective of the present work is to build a static geological model to be used to train students of the "Reservoir Geosciences and Engineering" master at IFP School.

A review of this first model is necessary to prepare a specific case study dedicated to education.

One of the objectives is to identify the main heterogeneities which may have an impact on fluid flow. A secondary objective is to simplify the existing model, keeping in mind the schedule of the training period which is limited to a duration of 3 weeks.

The available data base consists of:

180km^2 of 3D seismic data

Well data (5 wells) logs and core data
Porosity/permeability core measurements
Interpretation of Phi-K laws and well tests
Pressure data
Production history.

The main part of the project is done using the Petrel software for geological modelling (seismic interpretation, construction of the pillars and grids, property distribution) and the Easytrace software for well interpretation (definition of electrofacies and correlations).

The workflow of the complety static reservoir study is presented in Figure 1.2. and described in details in the chapter 4 of methodology.

My work began with a review of the literature of the regional geology where the FC Field is located. The second part consisted in checking the work realized in 2011 in order to define the adjustment to be made in each stage of the geological model.

In the third part, the structural model was built by interpretation of Derro, Upper Rutbah and Mulussa F dolomitic Formations and three different fault trends in the seismic data.

Then, I worked on the construction of the sedimentology model using well core information to define the environment of the Rutbah Formation deposition and interpretation of well logs to define electrofacies and Maximum Flooding Surfaces (MFS) of the units. Afterwards, a stratigraphy model was built by defining the palegeography of the Mulussa F and Rutbah formations and correlation of the wells. Finally, I integrated all the models carried out and make an each of this stage was quality-checked and update during this project.

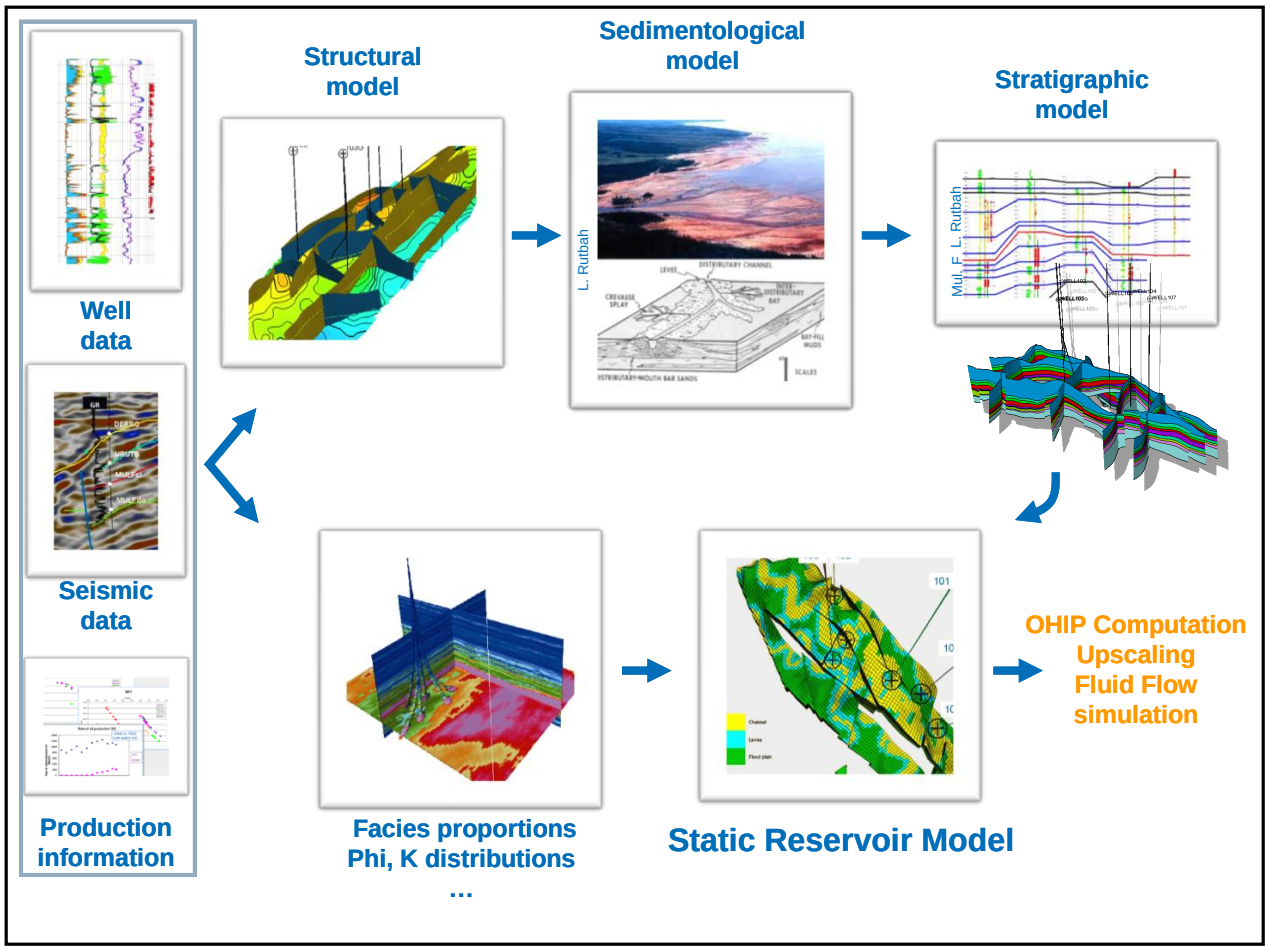

Figure 1.2: Workflow of the static model of FC, showing the most important stages for the construction of the geological model.

2. PRESENTATION OF THE CASE STUDY

The Euphrates graben system is one of the most petroliferous basins in Syria and it is recognized as a part of the Late Cretaceous rift structures developed in south - eastern Syria. This structure is an aborted continental rift and is described as a junction between the Palmyrides fold belt and the Euphrates depression (Litak et al., 1997). It is currently buried by up to 2.5 km of Cenozoic sedimentary rocks, (Olewcxynska., 2005).

In the FC field there are two reservoirs, one deposited in a deltaic environment called Rutbah Formation (Lower Cretaceous) and another one in a continental environment Mulussa F Formation (Upper Triassic); there are at least two fault trends affecting the reservoirs, generating compartmentalisation (Koopman., 2005).

2.1 GEOLOGICAL SETTING

Syria is located on the northern flank of the Arabian plate and the diverse structural and stratigraphic evolution of the area reflects a complex interaction between Cenozoic plate boundaries and pre-Cenozoic structures (Bydoun, et al., 1977). The Euphrates graben is situated at the southeast of Syria.

Syria is bordered by continent/ continent collision of the Arabian Plate converging to the Eurasian Plate at rate of 18±20 mm per year in an approximate direction of north - north-westerly (McClusky et al., 2000). As a result of this collision, the active transform and the convergent plate boundaries are currently proximal to Syria. (Brew et al., 2001.)

In Syria four major tectonic zones and intervening structural highs can be recognized (Barazangi et al., 1993). Most of the tectonic deformation throughout the Phanerozoic was accommodated in these zones – the Palmyride area, the Sinjar-Abd El Aziz area on the figure 2.1, the Euphrates Fault System and the Dead Sea Fault

System, where the intervening stable areas remained structurally high and relatively unchanged. The style of structural reactivation during the evolution has been linked to the orientation of the tectonic zones with the previous stress pattern. (Figure 2.1) (Brew et al., 2001).

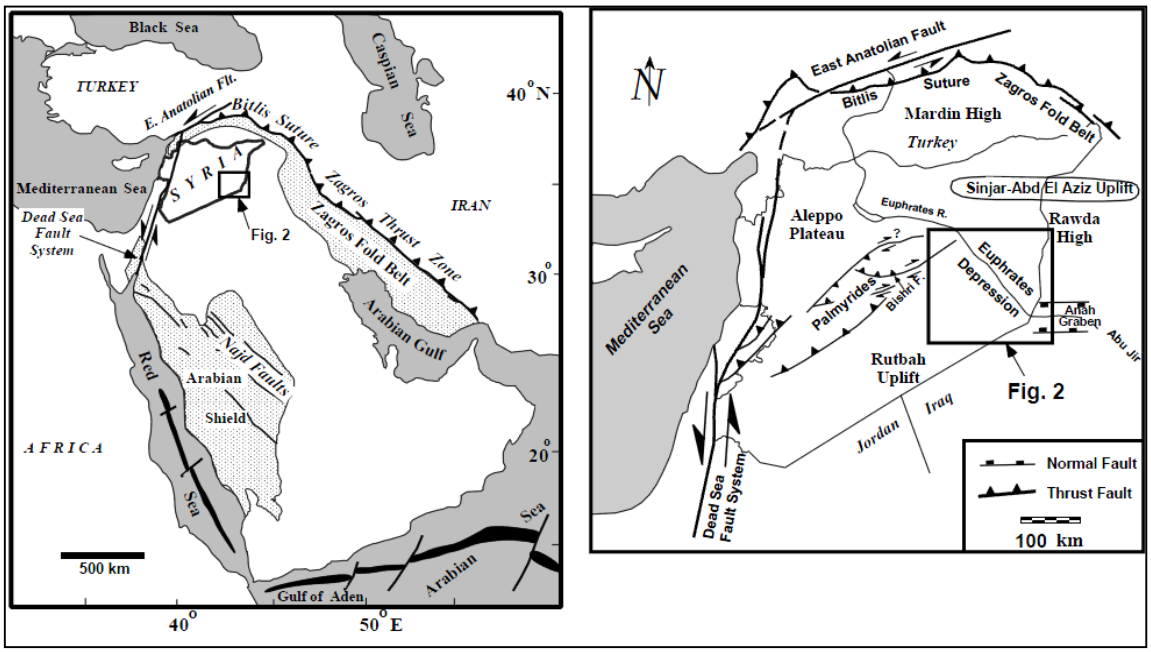

Figure 2.1: Generalized tectonic setting map of the Arabian plate. Hashed areas represent the main structural features in Syria. Note that Syria is almost completely bordered by plate boundaries. From Litak 1998.

Stampfli et al. (2001) presented a regional reconstruction of the evolution of the Tethys and eastern Mediterranean, although the issue is still under debate. Brew in 2001 described the agreements with Stampfli et al., 2001. In the current project this reconstruction is taken into account. For this reason, I give below a short description of the reconstruction with more focus on the Triassic and Cretaceous periods since the reservoirs were deposited during these ages. The Euphrates Graben was also developed in the Upper Cretaceous. The generalized chrono-stratigraphic chart is shown in figure 2.2 and described in the text.

Proterozoic (>545 Ma) to End Cambrian (495 Ma)

During the Pan–African orogeny the Southern Arabian plate was formed through Proterozoic accretion of island arcs and microplates against northeast Africa

between around 950 Ma and 640 Ma (Beydoun, 1991). In the Arabian shield there are well-exposed suture zone relics from this accretion, as well as the Najda-style fault which was produced when these sutures were reactivated. (Stoeser and Camp, 1985). The tectonic evolution of Syria throughout the Phanerozoic appears to have a strong influence as seen by the reactivation of this former crustal weakness zones. Brew 2001.

Subsequently, from about 620 Ma and 530 Ma, continental rifting and intracontinental extension followed the accretion on the area. Strike-slip movements on the Najd fault system, synrift deposition during infracambrian and Early Cambrian characterized this period (Husseini 1989). According to Husseini these synrift and postrift deposits resulted from the 'Jordan Valley Rift' which formed between Sinai and Turkey during the Infracambrian age (Brew 2001).

In the Paleozoic section there are many unconformities, one of these is at the top of the Cambrian where an erosional unconformity is recognized. This was created when relatively shallow water covered much of the Arabian plate. Brew 2001.

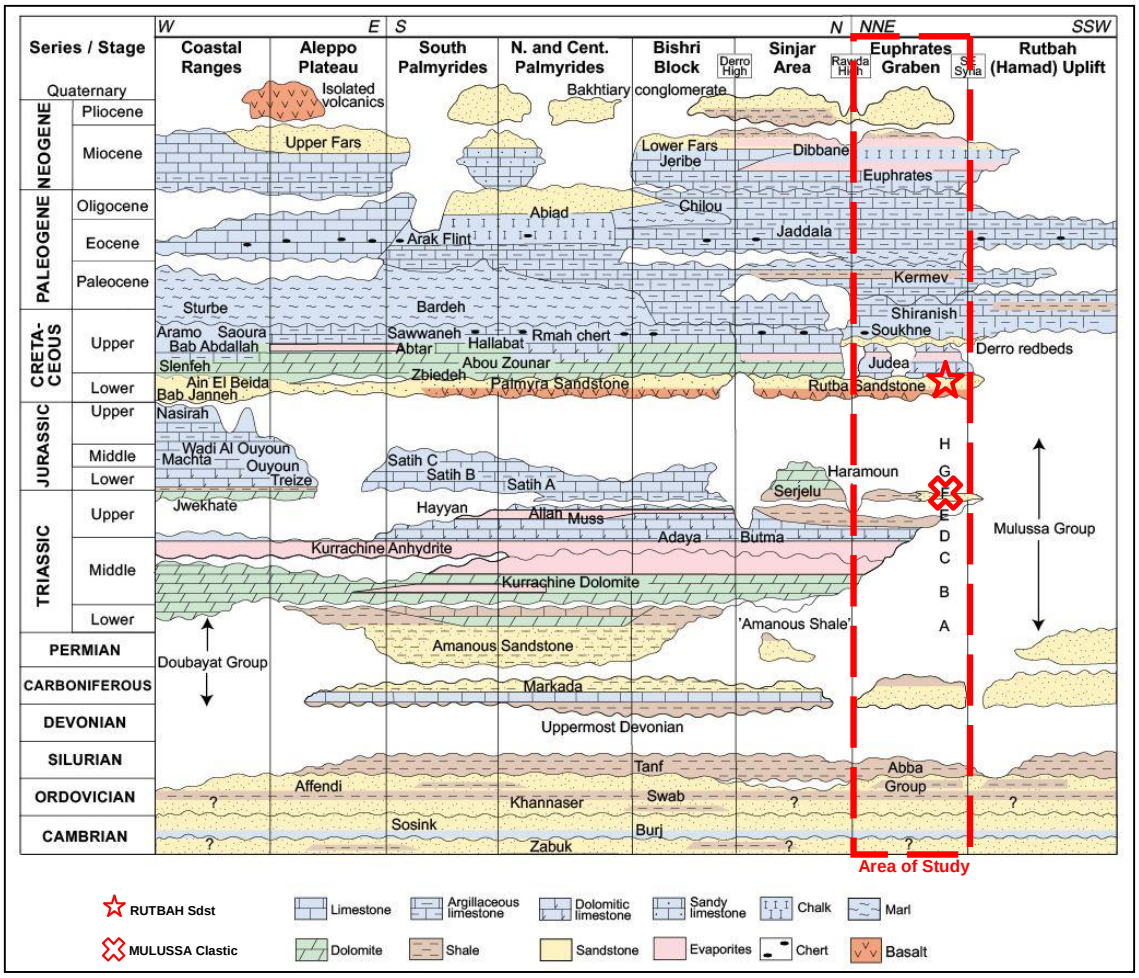

Figure 2.2: Generalized lithostratigraphy of Syria, (time intervals not to scale). Modified From Brew et al., 2001.

Ordovician (495 Ma) to Early Silurian (428 Ma)

The Ordovician section was deposited across a wide epicontinental shelf, which presented good development on the northern and eastern margin of the Arabian plate, the thickness shows a difference between 1.6km and more than 3.5km (Brew 2001). The variations of the sandstone facies from the western part to siltstone and shale facies on the southeast of Syria indicate open marine conditions to the east. (Sharland et al., 2001). The main source areas of the clastic deposits and reworked sediments on the Paleozoic were from the Arabian and Indian Precambrian shield uplifts on the south and west location.

According to Sharland et al., (2001) the top Ordovician unconformity was related to the hinterland uplift in the western part of Saudi Arabia. The Rawda-Rutbah high in

the eastern part of Syria and the western part of Iraq were also exposed during the Late Ordovician and Early Silurian.

During the Late Ordovician polar glaciation took place in much of Gondwana, including western Arabia. Subsequently, during the Early Silurian, deglaciation has been recognized as having been caused by Gondwana migrating toward the tropics (Brew 2001). As a result, sea level rose and flooded much of the Arabian plate. Regionally these deposits are recognized as hydrocarbon source rocks due to their high content of organic material (Brew 2001).

Late Silurian (428 Ma) to Devonian (345 Ma)

Sediments from the Late Silurian are directly overlaid by Carboniferous clastic deposits, showing a major unconformity extended in the time on the area. At the same time, in the north of Gondwana strong tectonic and volcanism occurred. Some authors cite the cause of this regional compression as obduction of the Proto-Tethys on current Iran. (Husseini 1992); uplift on the flanks of Paleo-Tethys rifting (Stampfli et al., 2001) or a more localized thermal uplift event (Kohn et al., 1992).

In Arabia the strata of the Late Silurian and Devonian ages are almost totally absent. The Early Silurian shales were eroded afterwards. In Syria the strata of the Silurian are present in the elongated depocenter approximately along the trend of the current Palmyrides, and are thinned or absent toward the north and south (Best et al., 1993). This could suggest erosion on the structural highs which were located on the southeast and northwest of the Palmiryde-Sinjar Trough during the Early Silurian (Brew 2001).

Brew (2001), suggested that the Rutbah and Rawda uplifts were connected through most of the geologic time. Then, in the Late Cretaceous, the dissection by the Euphrates Fault System occurred. Several episodes of minor subsidence after uplift

in the Devonian are identified although the Rutbah and Rawda uplifts remained structurally high for the rest of the Phanerozoic. (Brew 1997).

Carboniferous (354 Ma to 290 Ma)

In central Syria the Palmyrides/Sinjar depositional trough was completely developed, and it continued to be the main depocenter in the area until the Late Creataceous, delimited by the Allepo Plateau at the northwest and the Rutbah–Rawda uplift in the southeast (Brew et al., 1999). Gvirtzman and Weissbrod (1984) interpreted the Carboniferous trough to be a wide crustal down-warping between anticlinoria identified to the north and south of Syria. Husseni (1992), suggested that Devonian-Early Carboniferous folding could have created the major Devonian hiatus observed in Syria (Brew 2001).

Permian (290 Ma to 248 Ma)

During the Permian age there were changes in regional tectonics due to the opening of the Neo-Tethys until the Miocene (Brew 2001). Stampfli et al. (2001) suggested that on the north and east margin of the Gondwana, oceanic spreading separated the Cimmerian superterrane, and also that in the Permian and Early Mesozoic rifting along the north of African margin was the second phase of extension that began in the Early Carboniferous (Stampfli, 2001).

Robert and Dixon (1984), justified the oceanic nature of the eastern Mediterranean region as a consequence of the Permian Triassic rifting, where the northward subduction of the Paleo-Tethys controlled the Triassic sea floor spreading in the eastern Mediterranean. On other hand, Brew 2001 suggested that in the Late Permian the Palmyride Trough was developed by extension along the northern African margin enabling the sea-floor to spread to the Eastern Mediterranean.

This stratigraphic relationship shows that the Appelo Plateau and the Rutbah Uplift emerged throughout the Permian, possibly as uplifted flanks of the rift (Stampfli

2001). Brew (2001), affirmed that the rifting controlled a major part of the Permian-Triassic deposition.

Triassic (248 Ma to 206 Ma)

During the Permian–Triassic there was a regional change from the E-facing to W-facing passive margin (Best et al., 1993). This margin development is related to the continued postrift subsidence in the Palmirydes, as well as the fact that the synrift deposition in the Palmyride Trough appears to have continuity into the Early Triassic. The uppermost synrift sequence is represented by the Mulussa A Formation, described by Brew et al., (2001) as sandstones and shales with an increasing amount of dolomite and dolomitic limestone upward through the succession in central Syria. See Figure 2.3, which shows the generalized sedimentation and distribution of the facies during this time.

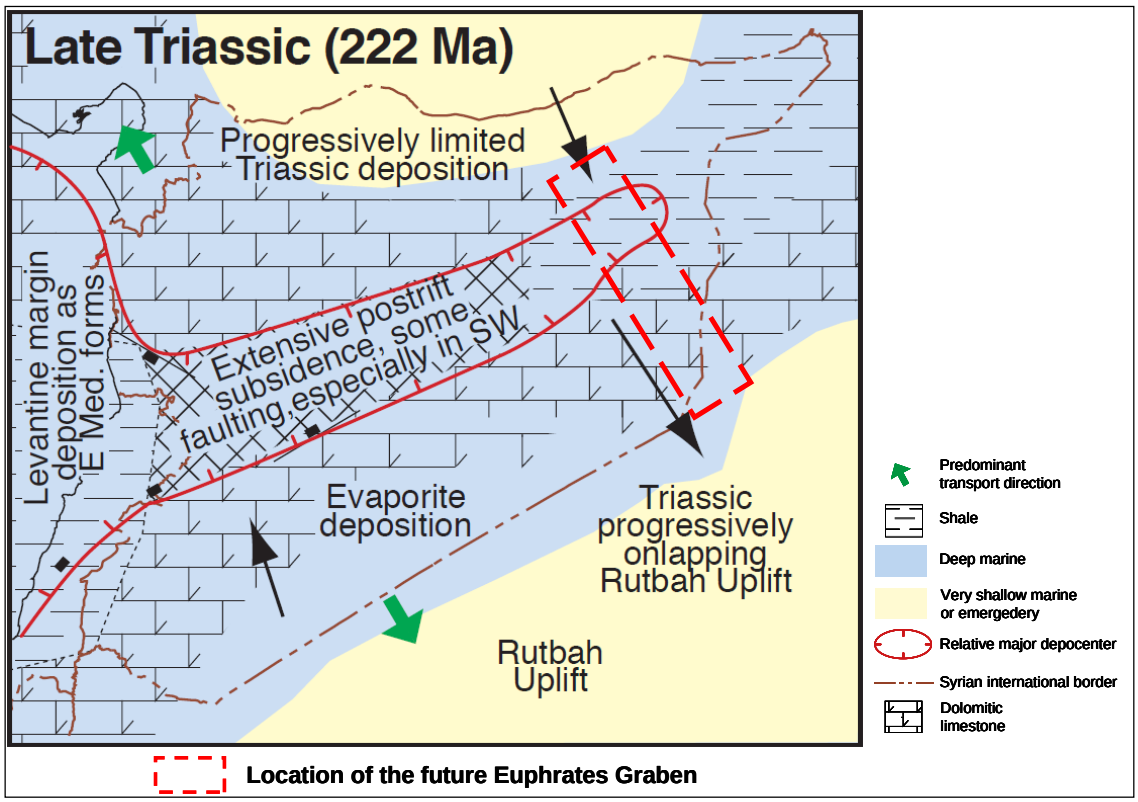

Figure 2.3: Syria sedimentation and facies deposition during Late Triassic. From Brew et al., 2001.

Rifting in the Palmyrides had ceased by the end of the Early Triassic while on eastern Mediterranean spreading was still active. Cohen et al. (1990) suggested that due to

the removal of the eastern Mediterranean spreading ridge along the Levantine transform faults, the Palmyrides rift stopped.

Extensive Early Triassic unconformity in most of Syria demonstrated the cessation of the Palmyrides rifting, and this is related to postrift unconformity and extremely low sea levels (Haq et al., 1988). The only exception recognized in the area corresponds to Central Syria where the sequence in the Permian through the Middle Triassic is conformable due to being the deepest depocenter in the area. This part then continued to be submerged while the others were exposed and eroded (Brew et al., 2001).

The deposits of the Middle Triassic correspond to dolomitic and limestone succession with some pelagic fauna (Mulussa B) and are spread spatially over most of Syria and are demonstrated by the succession of a deeper water environment. These deposits were the result of drift of the Arabian Plate in lower latitudes and the absence of source areas after plate organization. Then deposition on the Triassic started to be progressively limited to the internal Palmyride/Sinjar Trough though time and some minor sea level changes were registered on a pseudo-flat platform (Sawaf, 2001).

In the southeast of Syria there is an exception to progressively restricted Triassic deposition, where the Triassic strata onlap around along the axis of the Euphrates Fault System. The sediments of the Mulussa Group gradually onlap the Rutbah-Rawda Uplift to the southeast (Figure 2.3). The total sequence of the Triassic is found near the Bishiri Block, although the Mulussa F is only found in the southeast part. In the southeast of Syria the Triassic sequence onlaps the Carboniferous and Silurian strata on the emerged Rutbah –Rawda High.

Sawaf et al. (2001) and Stampfli et al. (2001) suggested a decreasing subsidence rate typical of post rift subsidence and showed that thermal relaxation probably continued until the Early Cretaceous. As a result, the dominant control of the Triassic depocenter was subsidence Brew et al.,(2001).

The emergence and erosion of the Aleppo and Rutbah-Rawda highs induced a sedimentary hiatus above the Triassic Mulussa F series. (Figure 2.2) (Brew et al., 2001). The Mulussa F presents different lithologies, which change from clay, siltstone and sandstone in contrast to the underlying carbonates and evaporites of the oldest formations. The clastics deposited on the Mulussa F formation were sourced from the Rutbah Uplift in the south and southwest that remained exposed during the Late Triassic. This formation marked the beginning of a regional transgression, which continued until the Early Jurassic. (Mouty, 2000).
The Al Hamad uplift is a NE-SW structure extending from the southwest Syria to the Euphrates Graben, which corresponds to the uplift in the Late Triassic. Jamal (2000) suggested that the fluvial sandstone of the Mulussa F Formation was sourced by the Al Hamad High instead of the Rawdah Uplift, which is far to the south as affirmed by Brew (2001).

The Rutbah high, in southwest Iraq, is composed of Permian to Cretaceous outcrops culminating over the present Paleogene–Neogene Al Hamad plain (Jamal, 2000). The absence of any phyllitic minerals, a metamorphic basement on the Mulussa F - which are characteristics of the Rawdah Uplift - could corroborate this suggestion. Figure 2.4 shows the Paleozoic basin uplift in the upper Triassic.

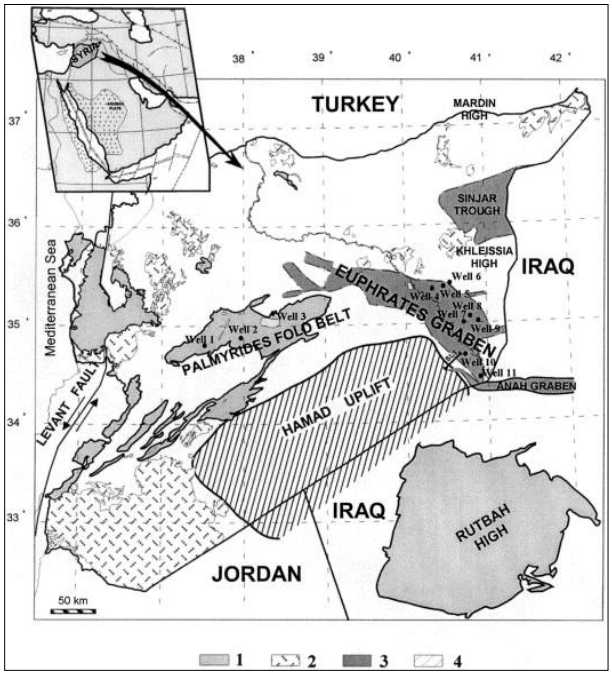

Figure 2.4: Palegeographic configuration of the Paleozoic Uplifts in Syria. From Jamal (2000). Syria

1. Mezosoic outcrops, 2. volcanic outcrops, 3. Mesozoic grabens hidden by Cenozoic burial. 4. Paleozoic basin uplifted in the Upper Triassic.

Jurassic (206 Ma to 142 Ma)

The transgression that began in the late Triassic and continued through the Early Jurassic spreading all over Syria except the Rutbah –Rawda (where the current Euphrates graben is located), and the Aleppo/Mardin high, that remained emerged during the Jurassic (Mouty, 2000). The sequence was characterized by limestone, dolomite and occasionally marl. (Mouty, 2000).

During the Jurassic, the Palmyride/Sinjar Trough extended through the southwest of Syria and Lebanon toward the still developing eastern Mediterranean (Walley, 2001). The reactivation of the Permian rift–bounding faults could also be responsible for the Jurassic faults found along the eastern Mediterranean margin. (Best et al., 1991)

The most pronounced regression identified in the Kimmeridgian was accompanied by widespread erosion and showed over most of Syria (Mouty, 2000). For this

reason Jurassic strata are only preserved in the deepest part of the Palmyride–Sinjar Trough.

The Late Jurassic, with continued volcanism through to the Aptian, has been recognized in the Anti-Lebanon, the Syrian Coastal Ranges, the Palmirydes, and others parts of the eastern Mediterranean. (Mouty et al., 1992). According to Laws and Wilson (1997), the relationship of volcanism, regional tilting, and uplift could be related to mantle plume activity centered in the Syrian region.

Early Creataceous (142 Ma) to Coniacian (86 Ma)

Into the Cretaceous a continuation of the Late Jurassic hiatus and erosion has been recognized. This regional unconformity and widespread Early Cretaceous volcanism over all the area suggest a continuation of mantle plume activity (Laws and Wilson 1997).

The regional Early Cretaceous transgression covered most of the area of the North Arabian platform with deposition of fluviodeltaic to shallow marine sandstone and shales.

Early Cretaceous to Cenomanian Rutbah sandstone in eastern Syria has equivalent Aptian and Pre-Aptian members in the Palmyride area. (Mouty and Al-Maleh, 1983). Nevertheless, the only area that was not covered by the Rutbah sandstones or equivalent was the Rutbah–Rawda uplift because this area was still exposed, as it had been for most of the Phanerozoic. For this reason Cretaceous sandstones could have come from the erosion of the Carboniferous and Permian sandstones.

Paleogeographic conditions could be defined by the variation of the facies from the south with sandstone to more shaly and carbonaceous deposits to the north, showing the increasing distance from the source to the Rutbah Uplift. (Brew 2001). The Cretaceous and Jurassic formations of show clear trends suggesting deeper water, less–restricted circulation, and a smaller proportion of clastics in the west

and southwest (Mouty 1983). Figure 2.5 shows the paleogeographic configuration and the dominant facies during Aptian age.

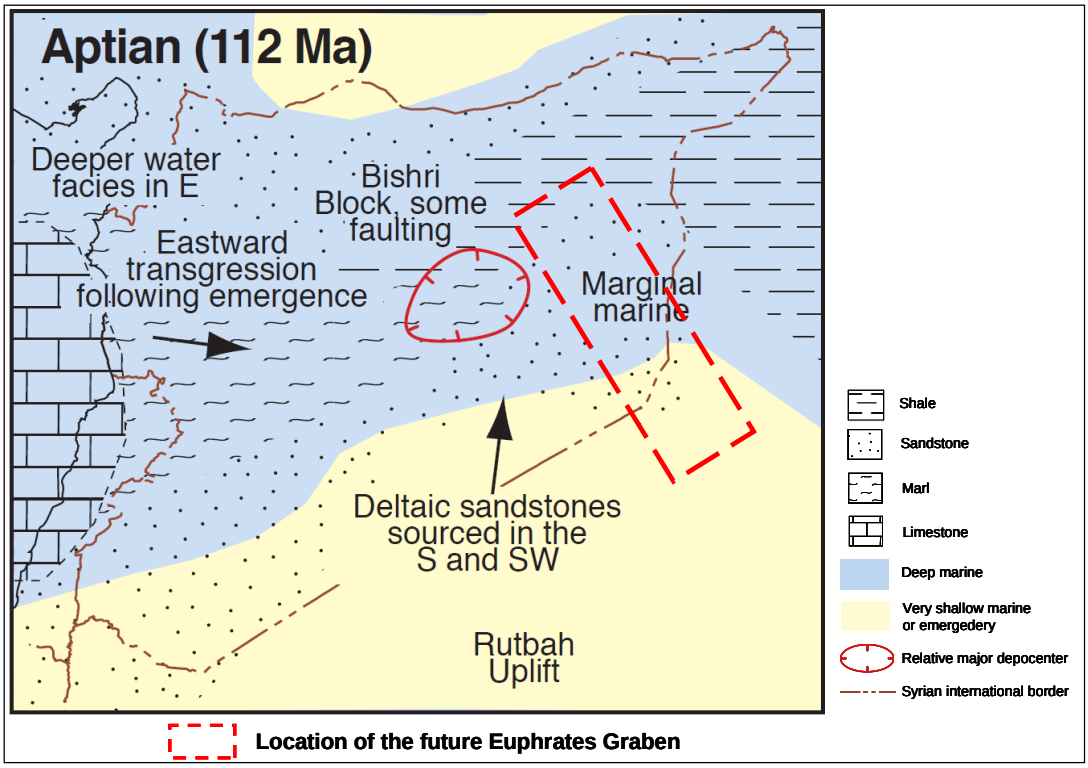

Figure 2.5:Dominant facies and sedimentation during the Aptian age, which correspond to Rutbah Formation deposition.

For instance, in the Euphrates Graben, located in eastern Syria, the deposition of Cenomanian-Turonian Judea Limestone corresponds to marginal to shallow water depths, which indicates a calm environment of deposition – instead of the equivalent Palmyride strata, which show medium to shallow depth marine deposit conditions

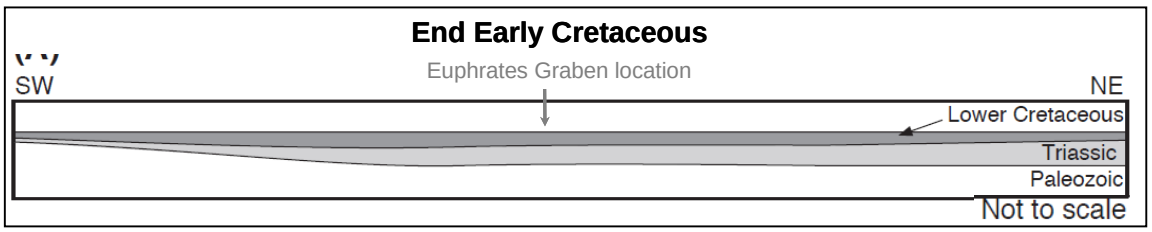

Figure 2.6: Schematic SW –NE cross section at the End of the Early Cretaceous, before the formation of the Euphrates fault system. Dark grey represents the latest deposition. From Litak et al., 1998.

Formation of the Euphrates Fault System.

In the Turonian–Coniacian period the Euphrates rifting activity occurred. It was registered as a widespread unconformity and associated to volcanics and anhydrite deposits (Sharland et al., 2001). Initial heating and uplift of the lithosphere under conditions of initial rifting and plate flexure created the pre-rift unconformity, due to ophiolite obduction. Afterwards, red-beds deposition was restricted to eastern Syria (Derro Formation) and western Iraq (Figure 2.7).

There is still debate about the exact cause of the Euphrates rifting; although, the presence of the prerift unconformity and the volcanism might favor an active rifting scenario, which could be related to the Early Cretaceous phase of the plume activity observed in western Syria. (Brew et al., 2001).

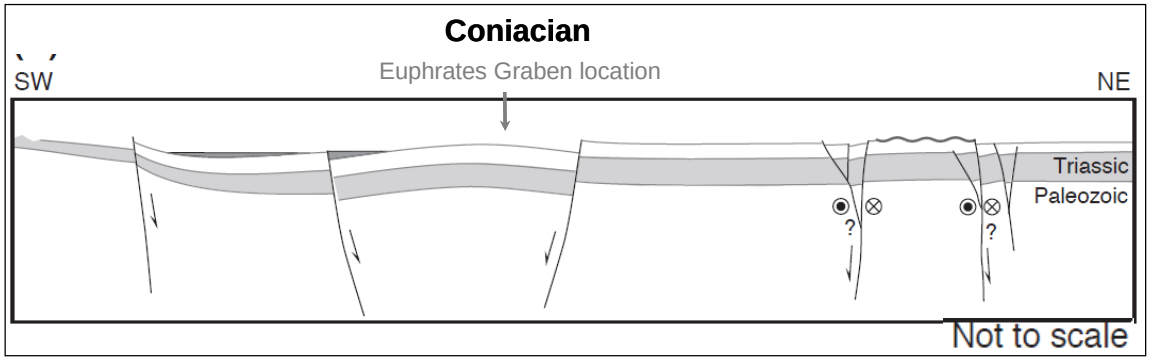

Figure 2.7: Schematic SW –NE cross section at the Coniacian, before the formation of the Euphrates fault system. Dark grey represents the latest deposition. From Litak et al., 1998.

Santonian (86Ma) to Campanian (71 Ma)

The Euphrates Fault system rifted across oblique-slip normal faults from the Santonian onward. However, the system was more active during the Campanian and early Maaschtrictian. Consecutive filling of the grabens during transgression occurred and the first was in the west with the Rmah chert Fm., continuing towards the east with the Derro redbeds. Gradually deeper water carbonate facies filled the graben with a thick sequence of pelagic and marly limestone named the Shiranish Formation (Brew et al., 2001). The Euphrates Fault System and Bishi depocenter were connected by a fault–controlled topographic low during this time.

Brew et al.,(2001), as well as Lovelock (1984), suggested that the Euphrates rifting was driven by slab-pull forces in the approaching subduction zone in the Neo-Tethys, where the tensional forces responsible for transtension in the Euphrates were transmitted across the Arabian Plate.

Maastrichtian (71 Ma to 65 Ma)

During the Maastrichtian, the thick Shiranish Formation continued to be deposited in the Euphrates Fault System. Some small indications suggest a reorientation of the stress direction and a decrease in the speed of the extension just before the final of the rifting. (Brew et al., 2001).

Litak et al. (1998), documented that strike slip is more common amongst the NW-striking faults in the Euphrates deformation than amongst the WNW-striking features. In addition, the faulting stopped before the end of the Cretaceous. An unconformity is registered in the Shiranish Formation (Litak et al., 1998). The reorientation of extension from SW–NE to N-S in conjunction with changes in extension in the Abd el Aziz-Sinjar area and in the Neo-Tethys subduction could be the explanation of these observations (Litak et al., 1998). Figure 2.8.

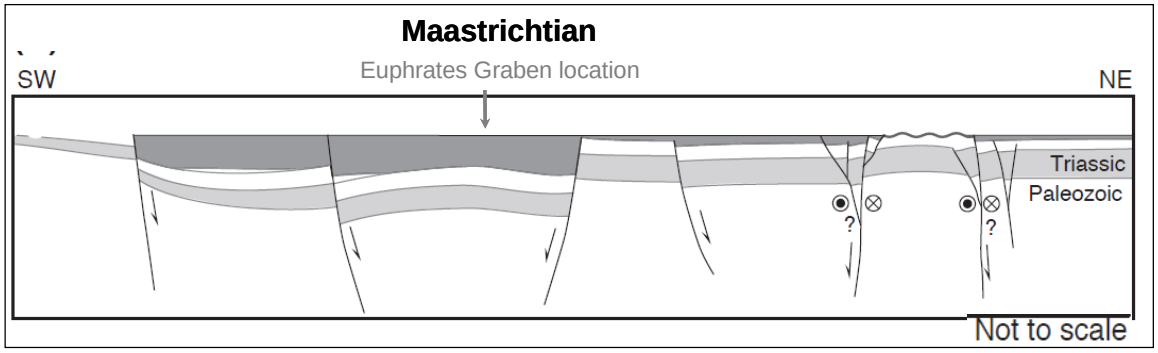

Figure 2.8: Schematic SW–NE cross section at the Maastrichtian age, when the faults of Euphrates graben stopped. Dark grey represents the latest deposition. From Litak et al.,1998.

Paleocen (65 Ma) to Oligocen (24 Ma)

In the Euphrates graben, widespread thermal subsidence followed the Late Cretaceous rifting. At this time the basin was progressively shallowing. For this

reason the Paleocen Kermev Formation in the Euphrates graben contains more chert than the underlying Shiranish Formation. Very minor transpression in the Euphrates Fault System has been observed at this age. Figure 2.9 shows the cross section at this time.

The plate-wide compression is explained by Hempton (1985) as the initial period of the final collision of the northern Arabian plate in the Middle to Late Eocene. This event could be responsible for the compressional tectonic events in the area.

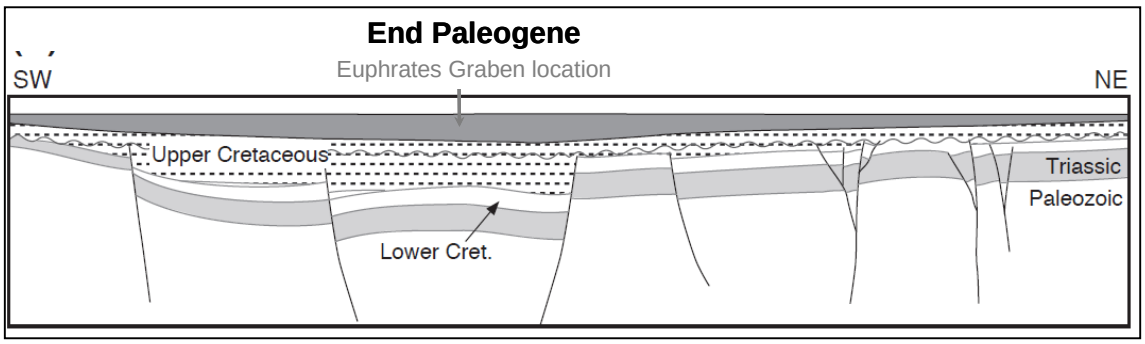

Figure 2.9: Schematic SW–NE cross section at the End Paleogen age during thermal subsidence of Euphrates graben. Dark grey represents the latest deposition. From Litak et al., 1998.

Miocen (24 Ma) to Holocen

The final transition to continental conditions in Syria is documented in the Miocene age. Although this event was progressive over the Arabian plate, due to the partitioning by tectonic uplift, more open marine conditions prevailed to the northwest throughout the Miocene and Pliocene (Brew et al., 2001).

The Middle to Late Eocene suturing of Africa–Arabia to Eurasian was accommodated in part by the shortening and thickening of the Arabian continental margin. (Hempton, 1985).

The stress created by the moving during convergence continued to form the compressional features initiated in the mid-Late Eocene, but at a slower rate. However, this stress regimen was modified by the beginning of continental stretching and rifting in the Red Sea in the Late Oligocene – Early Miocene. (Brew et al., 2001)

In the Mid-Late Miocene the terminal suturing of Arabia to Eurasia occurred. Meanwhile the Late Miocene is marked as a period of increasing compression in Syria, caused by the end of the shortening along the northern margin. As a result, basin inversion of the Palmyride fold and thrust belt (Chaimov et al., 1992), was accelerated and minor shortening occurred in the northwestern part of the Euphrates Fault System (Litak et al., 1997). (Figure 2.10)

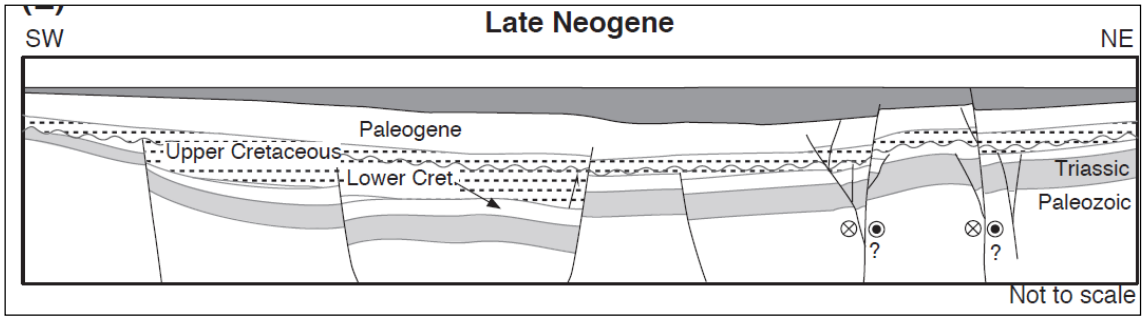

Figure 2.10: Schematic SW–NE cross section of the Late Neogene in North-west minor shortening and inversion of the Euphrates fault system. Dark grey represents the latest deposition. From Litak et al., 1998.

After the Late Pliocene, full-scale inversion did not take place on the Abd el Aziz structure (Brew et al., 1999). Inversion in the Euphrates Fault System is very minor and transpression was limited to the northwest segment of the system. This could be explained as a consequence of the Abd el Aziz–Sinjar structures accommodating most of the late Cenozoic strain. Moreover, the oblique orientation of the Euphrates Fault System, formed in relation to the Alpine collision, favors strike slip reactivation that is difficult to recognize at the surface. Pinokarov (1966), also suggested that the aborted grabens are still actively inverting. Figure 2.11

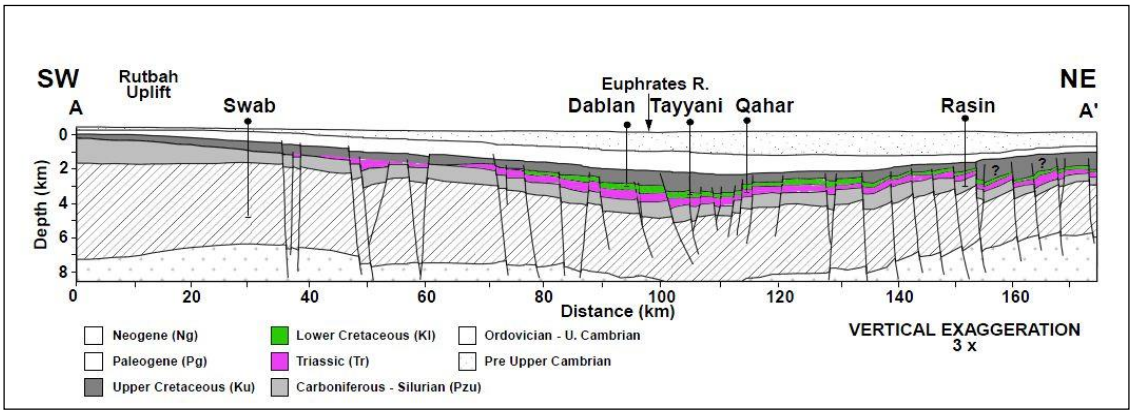

Figure 2.11: Structural SW-NE cross section across the Euphrates graben system. Location is presented in figure 1.1. Edited from Litak et al., 1998.

2.2 PETROLEUM SYSTEM

The biggest onshore hydrocarbon play in Syria is the Euphrates graben, where more than 400,000 barrels of light, sweet crude are estimated to be produced daily from the graben, corresponding to around 520,000 barrels on the national average. (Oil & Gas Journal, December 2000). Estimation of the proven recoverable reserves in the Euphrates area are around 1 billion barrels of oil and much lesser amounts of gas. (OAPEC Bulletin, 1996)

The primary production is mainly provided by the Lower Cretaceous Rutbah Sandstone (Figure 2.11). The Rutbah Formation was deposited during the Neocomian transgression in eastern Syria. It has a high porosity (estimated up to 20%), and well-maintained permeability (Brew 2001, Litak 1998). Additional reserves are associated within the Late Triassic Mulussa F fluvial sandstones, which were deposited in the Upper Norian within a regressive continental sequence in the Euphrates graben (Jamal 2000).

The source rock is principally the Upper Cretaceous marly limestone Soukhne and Shiranish formations with up to 1.7% TOC. These source rock were widely in eastern Syria (Brew 2001), although others are registered in the Silurian Tanf Formation (Figure 2.12), and possibly within the Carboniferous formations (Ruiter et al., 1994). The productive trend follows the fault trends of the graben axis. The production could be governed by the thickness and maturity of synrift source rocks because most of the fields are located in these areas (Litak et al., 1998)

The seal of the system is the thick Shiranish section which provides closure both above and laterally, achieved against the normal faults (Litak, 1998). In addition, the shaly Derro clastics have been proven to be a good seal (Beydoun, 1991). (Figure 2.12)

The traps are located on structural highs associated with normal faults, and generally formed by the latest Cretaceous normal faulting that created the rotated fault-block traps where the Rutbah sandstone is juxtaposed against the marly shales of the Shiranish Formation.

The trap integrity is affected only in the areas that have experienced significant reactivation in the northwestern part of the Euphrates fault system.

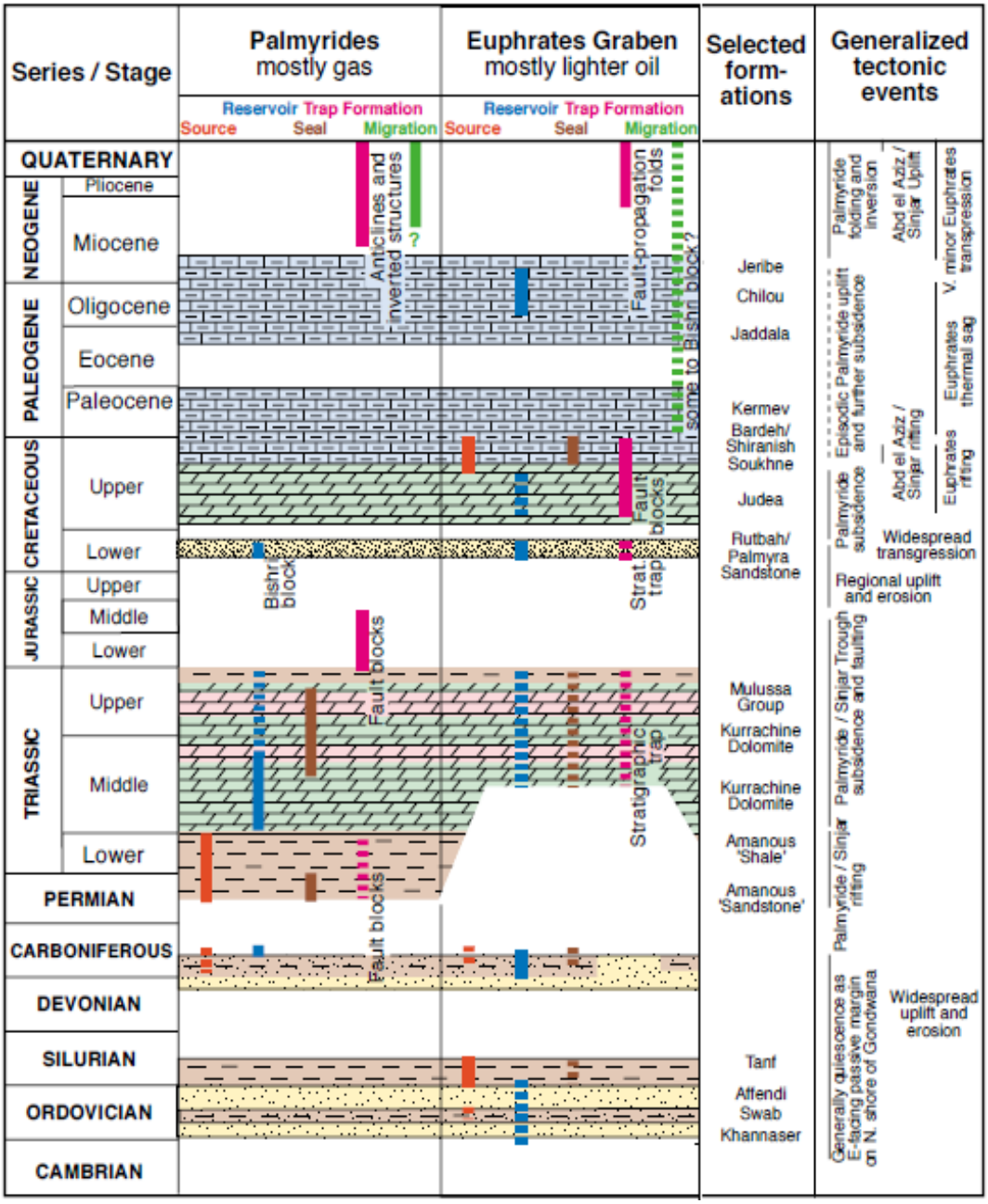

Figure 2.12: Generalized stratigraphy and selected structural elements in the Palmyrides and Euphrates graben hydrocarbon provinces of Syria. Solid lines show certain elements in the system, dashed lines show uncertainties. Modified from Litak et al., 1998.

3. METHODOLOGY

In the construction of the geological static model the source data for the workflow are seismic data, well data and production information. The main stages consist in the construction of the following models (see Figure 1.2):

1. the structural model, which defines from well tops and seismic data the structural framework of the reservoir in terms of faults and horizons,
2. the sedimentological model, based on the sedimentological facies interpretation of available core data and well logs, which leads to sedimentary environments and proximal-distal organisation of the depositional profile,
3. the stratigraphic model, built from the well to well correlation of time lines and the vertical organization of facies associations using the sequence stratigraphy concepts, which defines the main litho-stratigraphic units to be taken into account in the static reservoir model. These units are gridded to build the static reservoir model,
4. the computation of parameters to be used to fill the static reservoir model with properties such as facies, porosity, permeability,
5. the filling of the static reservoir model. This stage requires a deterministic or stochastic method to distribute the properties from the wells to the inter-well domains of the grid. The litho-stratigraphic units are simulated independently because the parameters depend on sedimentology and sequence stratigraphy. In some specific reservoir cases, the seismic data can be used to better constrain the simulation of reservoir properties.

In the first stage of the present project I performed a quality control (QC) of the original data, an interpretation made by the students in 2011 (2011 model), and on the results obtained. I then defined of the adjustments necessary to improve and simplify the previous model. A new model was then built with the same database.

In this chapter the QC for the previous structural, sedimentological, stratigraphic and static reservoir models is presented (see workflow in figure 1.2). Results obtained after improvement are presented in chapter 4. Throughout the process, I performed quality control even going backward to refine the structural model, the stratigraphic model and the geological model in order to achieve a realistic static model which will facilitate the history matching of production data.

3.1 Structural Model

3.1.1 Dataset

For the construction of the structural model the available data were: a 3D pre-stack time migration equalized (PSTM) seismic survey of 180km2 (Figure 3.1). For the lithologic calibration of seismic stratigraphy: Velocity Seismic Profile (VSP) – Check shots (CS), Sonic and density logs, and also a synthetic seismogram of well 103. For time–depth conversion: Volume of VRMS on the field. In addition, one horizon of the Paleozoic age interpreted on time was given with the data set.

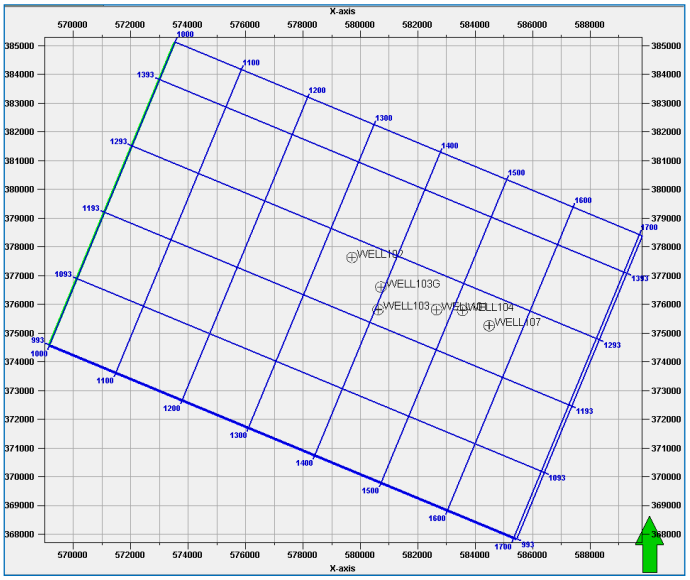

Figure 3.1: Location of the seismic volume, and wells.

3.1.2 Quality check of the 2011 model

Horizons

The project created on Petrel software 2011 by the students was the reference for the QC. They interpreted 6 horizons: Euphrates, Aliji, Shiranish, Upper Derro, Upper Rutbah and Mulussa F dolomite (see Figure 3.2). I focused on the horizons related to reservoir and seal formations, and for this reason the QC was only performed on the Upper Derro, Upper Rutbah and Mulussa F dolomite horizons. See table 3.1 details of the main horizons and surfaces using in the project.

Formations	Horizons TWT	Surfaces TWT	Surfaces Depth
Top Derro	Derro	Derro	Derro
Top Upper Rutbah	Upper_Rutbah	Upper Rutbah	Upper Rutbah
Top Mulussa Fdo	Mulussa F dolomitic	Mulussa F dolo	Lower Rutbah
			Mulussa F clas
			Mulussa F dolo
Paleozoic	Paleozoic	Paleozioc	Paleozoic

Table 3.1: Surfaces–Horizons have been used during the 2013 model.

Even if the Paleozoic Top was not drilled in well 103, which is the well that was used to tie the tops with the seismic cube, it is given in the data set and presents good continuity on the entire area. The Rutbah and Mulussa F clastic formations are difficult to follow through the area due to the seismic characteristics and low contrast between acoustic impedances.

The Mulussa F dolomitic and Upper Rutbah tops interpreted by the students correspond to a shift in the Paleozoic horizon with a constant value (Figure 3.2, 3.3). This is why the intervals between the surfaces created (Rutbah and Mulussa F dolomite) have a regular thickness. A different case is seen in the Derro formation which was interpreted as an erosional surface for each 20 in-lines and 20 cross-lines on the seismic volume. As a result, the underlying Rutbah Formation was eroded in the areas where the shifting pushed it higher than the Derro Formation.

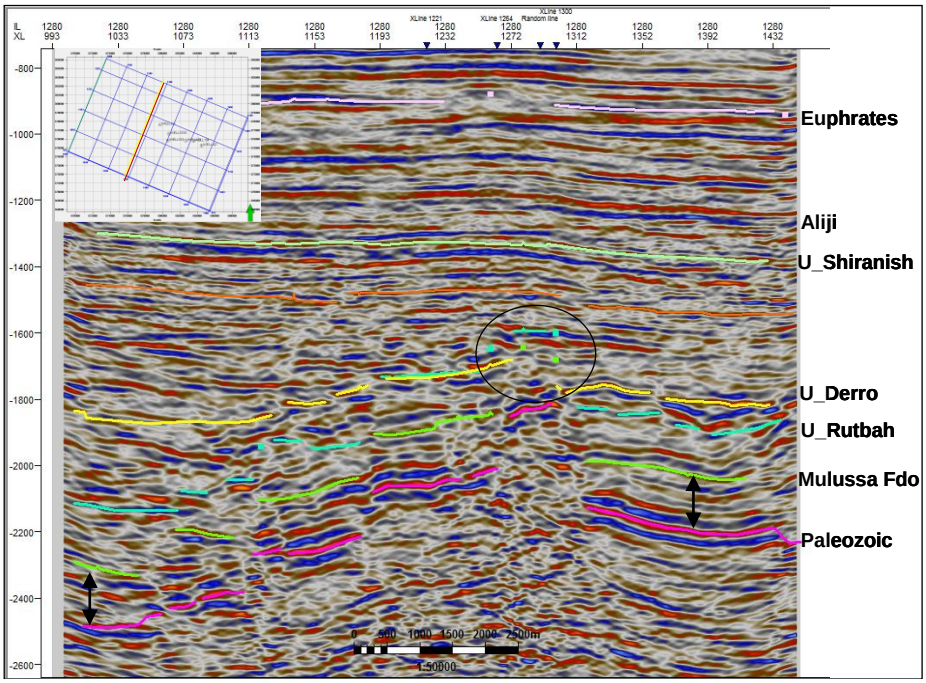

Figure 3.2:In-line 1280, Interpretation 2011 model, constant thickness of F dolomite and Upper Rutbah, in yellow erosional Upper Derro Formation. Note that horizons are crossing (circle): older formations are above younger one.

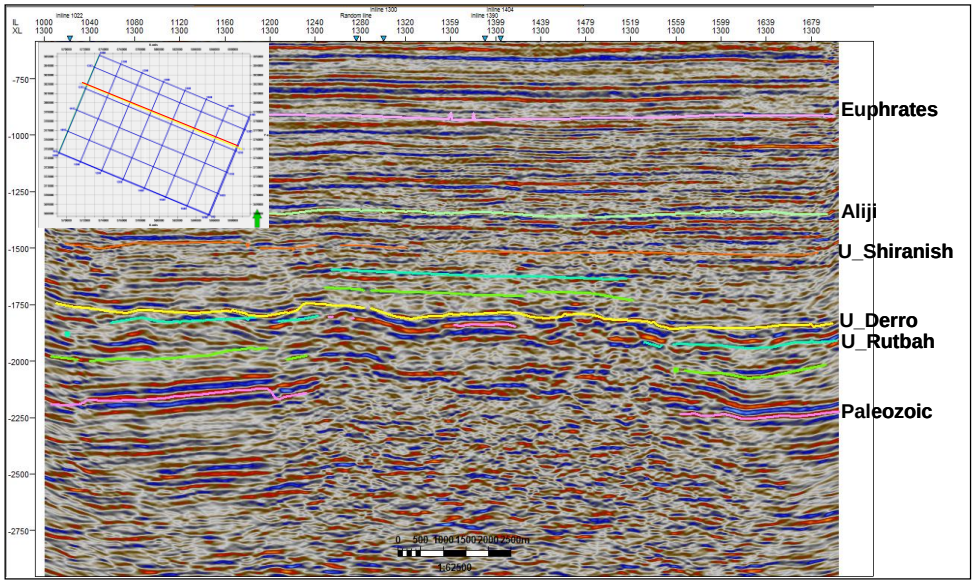

Figure 3.3:Cross-line 1300, Interpretation from 2011 model, Interpretation from students 2011, constant thickness of Mulussa F dolomite and Upper Rutbah, in yellow erosional Upper Derro Formation.

Faults

In the 2011 model, there were 3 main fault trends interpreted in the following directions: NW-SE, NNW-SSE and SSW-NNE (Figure 3.4). These faults were picked every 10 in-lines and 10 cross-lines but in different seismic lines than the horizons.

For this reason it is difficult to identify how the faults affected the horizons (Figure 3.5). The faults have short lengths resulting in two different segments in the vertical plane for the same fault.

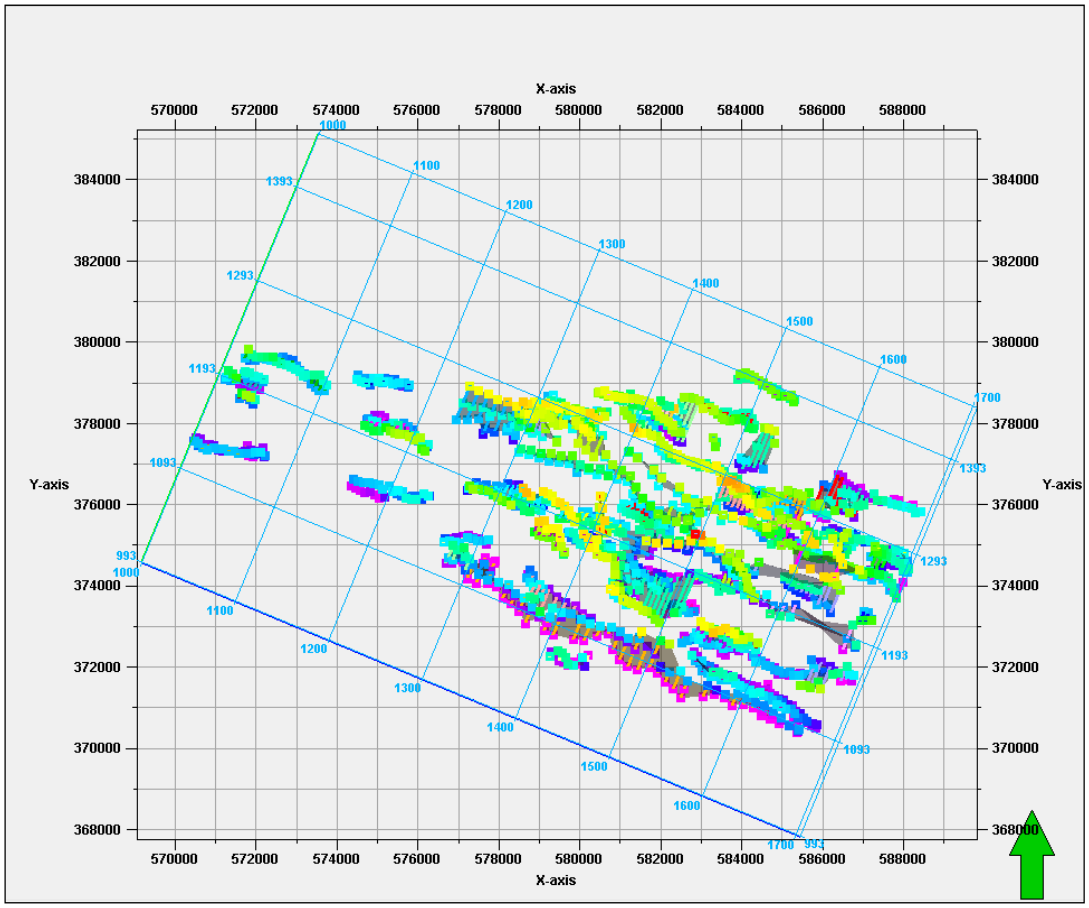

Figure 3.4: Top view of the trend of faults interpreted in model 2011, and final structural model on time.

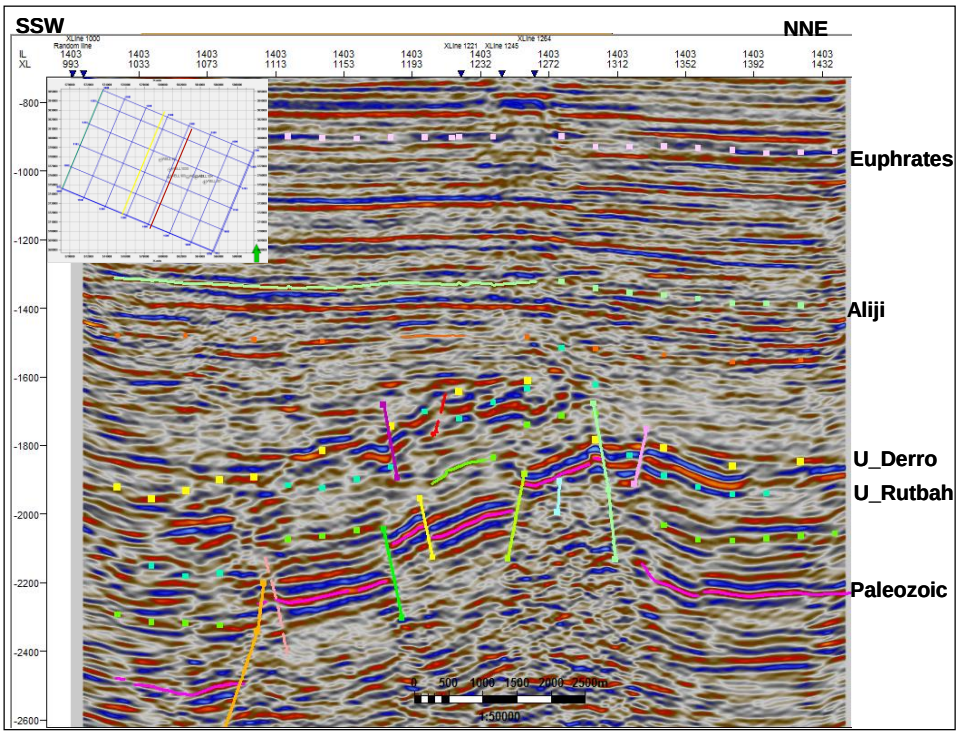

Figure 3.5: In-line 1403, faults interpreted by the students in different In-lines than the horizons. Notice that some faults are picked as two different segments when there could be continuation as the same fault.

Velocity model

In the data set the VSP check–shot from well 103 was given and was used for the velocity model created in Petrel. The students defined 4 zones in a layer cake model and used the Interval velocity (V0) as a constant with the gradient K constant in each interval. These values were calculated in the program using the cross plot and included in the model. Figure 3.6.

In the program the students defined the relationship of the zones as V=V0+K*Z, which is explained below:

At each location XY the velocity changes in the vertical direction by a factor of K. V0 represents the velocity at a reference datum (for example surface), and Z the distance from the same reference datum. (Internal document, IFP School). The K value is negative due to time and depth decreasing downwards. In Figure 3.7 there is a schematic description the arrangement and values used in the model.

This velocity model was used in a time–depth conversion of the surfaces and faults for the structural model, a process which was performed after pillar gridding.

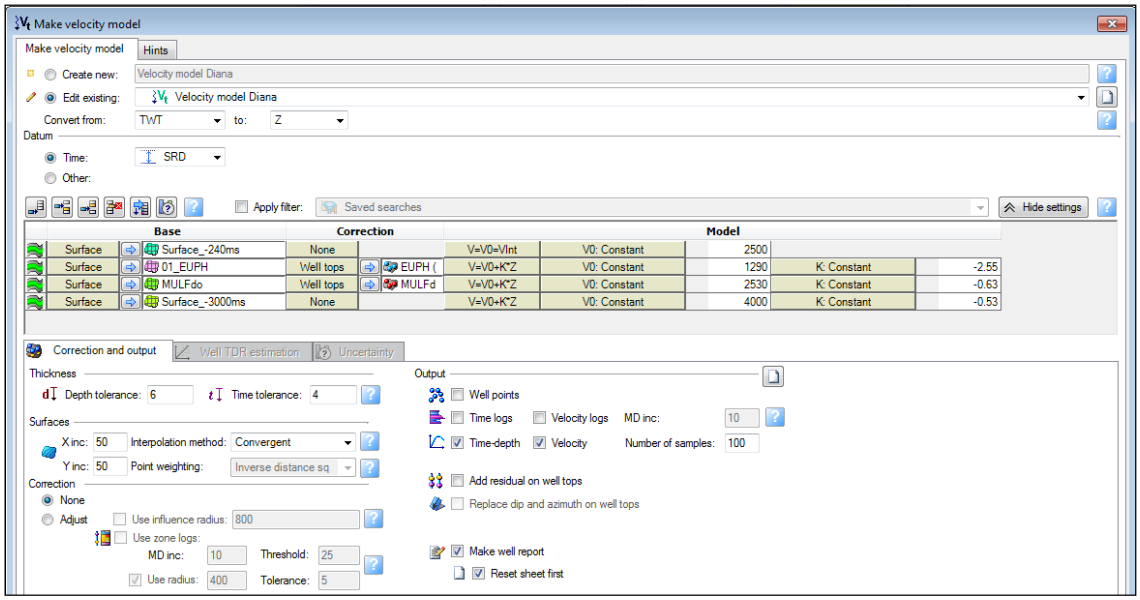

Figure 3.6: Description and values used in the velocity model for the time-depth conversion in Petrel.

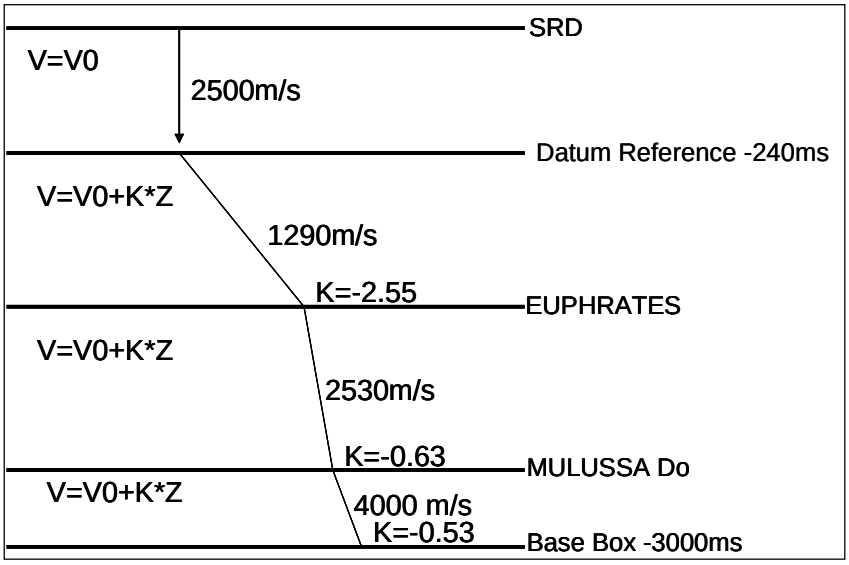

Figure 3.7: Schematic description of the velocity model created in 2011.

3.1.3 Improvements to be made

The main input for the structural model is the seismic interpretation and some weaknesses of the previous model were identified. A summary of the QC is presented in Table 3.2, and the details are explained below.

Horizons	Good	Acceptable	To be refined
Upper Derro		X	X
Upper Rutbah			X
Mulussa F_Dolomite			X
Trends Faults			
NW-SE			X
NNW-SSE			X
SSW-NNE			X
Time - Depth Calibration			
Well Check Shot			X
Velocity Model		X	

Table 3.2: Summary of the QC performed and decision of improvements to be made.

After checking the seismic interpretation made by the students, I decided to reinterpret the main horizons related to seal and reservoir formations. The picking was done for each 20 In-lines and 20 Cross-lines. As the tie of well 103 was unclear in the program, I started by the creation of a new synthetic seismogram in order to improve the time-depth conversion match and better identify the seismic reflectors with the wells tops.

This new interpretation was made in order to obtain a more realistic thickness of the formations instead of a regular thickness as in the 2011 project. More than one parameter influences the thickness of the reservoir. These are the palegeography at the time of deposition, the structural setting and also the erosion after deposition.

In addition, the structural framework was reinterpreted (every 10 In-lines and 10 cross-lines) in the same seismic lines as for the horizons. Longer faults where picked in seismic, patterns of deformation are visible on all formations and correspond to extension setting during the synrift stage in the Coniacian age. This deformation affected all the formations from the Paleozoic up to and including the Derro Formation.

In order to pick the faults and define the spatial extension some attributes were used such as extracted amplitude over the Paleozoic surface (Figure 3.8) where the main fault trends were identified and followed through the volume. The attribute of variance was also used with the same purpose to define the faults (Figure 3.9).

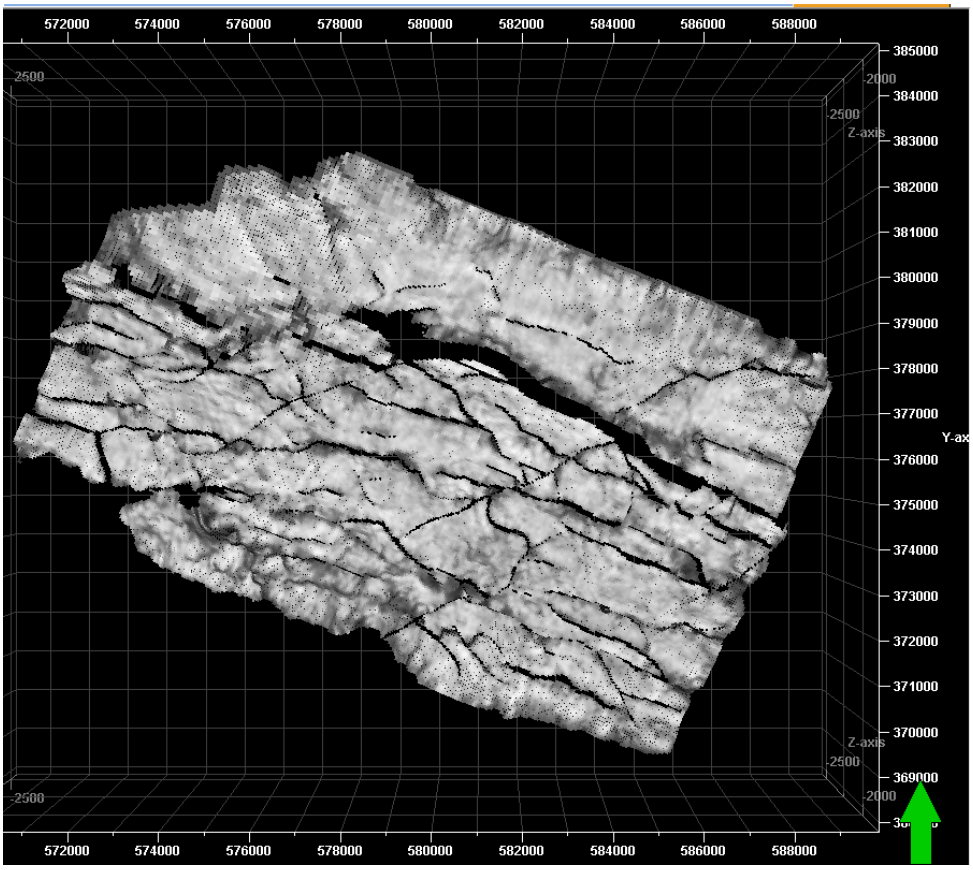

Figure 3.8: Extraction of amplitude over the Paleozoic horizon.

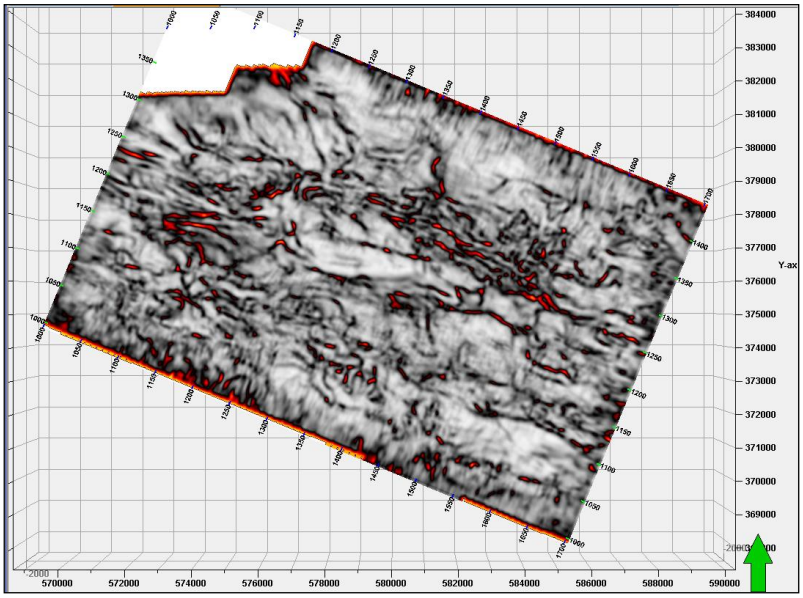

Figure 3.9: Time-slice (2000ms) showing the variance attribute used in the definition of the structural framework

In the velocity model created by the 2011 students the markers of the wells accurately match the converted time domain to depth domain. For this reason, no modifications were made to it. (Figure 3.10)

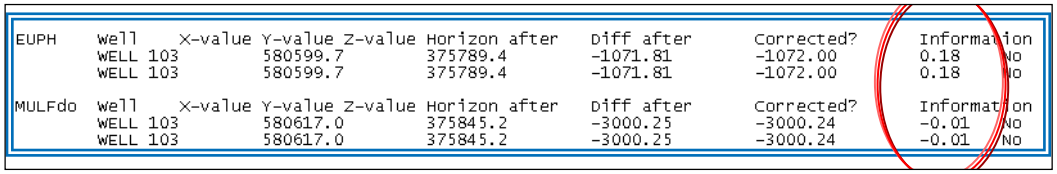

EUPH	Well	X-value	Y-value	Z-value	Horizon after	Diff after	Corrected?	Information
	WELL 103		580599.7		375789.4	-1071.81	-1072.00	0.18 No
	WELL 103		580599.7		375789.4	-1071.81	-1072.00	0.18 No

MULFdo	Well	X-value	Y-value	Z-value	Horizon after	Diff after	Corrected?	Information
	WELL 103		580617.0		375845.2	-3000.25	-3000.24	-0.01 No
	WELL 103		580617.0		375845.2	-3000.25	-3000.24	-0.01 No

Figure 3.10: Report of the error from Petrel with the velocity

3.1.4 Revised Interpretation

The results of the new interpretation of Derro, Upper Rutbah and Mulusa F dolomitic are presented in the chapter 4 of results as well as the faults framework on time and depth.

3.2 Sedimentological Model

3.2.1 Dataset

The available data to build the sedimentological model were: Raw logs (GR-SGR, SP, PEF, RHOB, NPHI, DT, Induction) and interpreted logs for wells 101, 102, 103, 103G, 104 and 107 (see location in figure 3.1); core data of well 102 in the interval of the Rutbah formation and facies definition in four wells for the Mulussa F clastic formation.

3.2.2 Quality check of the 2011 model

Mulussa F clastic Formation

The sedimentological model created by the students in 2011 reflects the information provided in the dataset, in which the Mulussa F clastic Formation is interpreted as a fluvial system divided in three facies: Channel, Levee and Floodplain. In combination with the interpretation of the electrical logs, the students defined that the packages

of sand correspond to Channels, shaly packages of sand to Levees and shale packages to Floodplain (Figure 3.11).

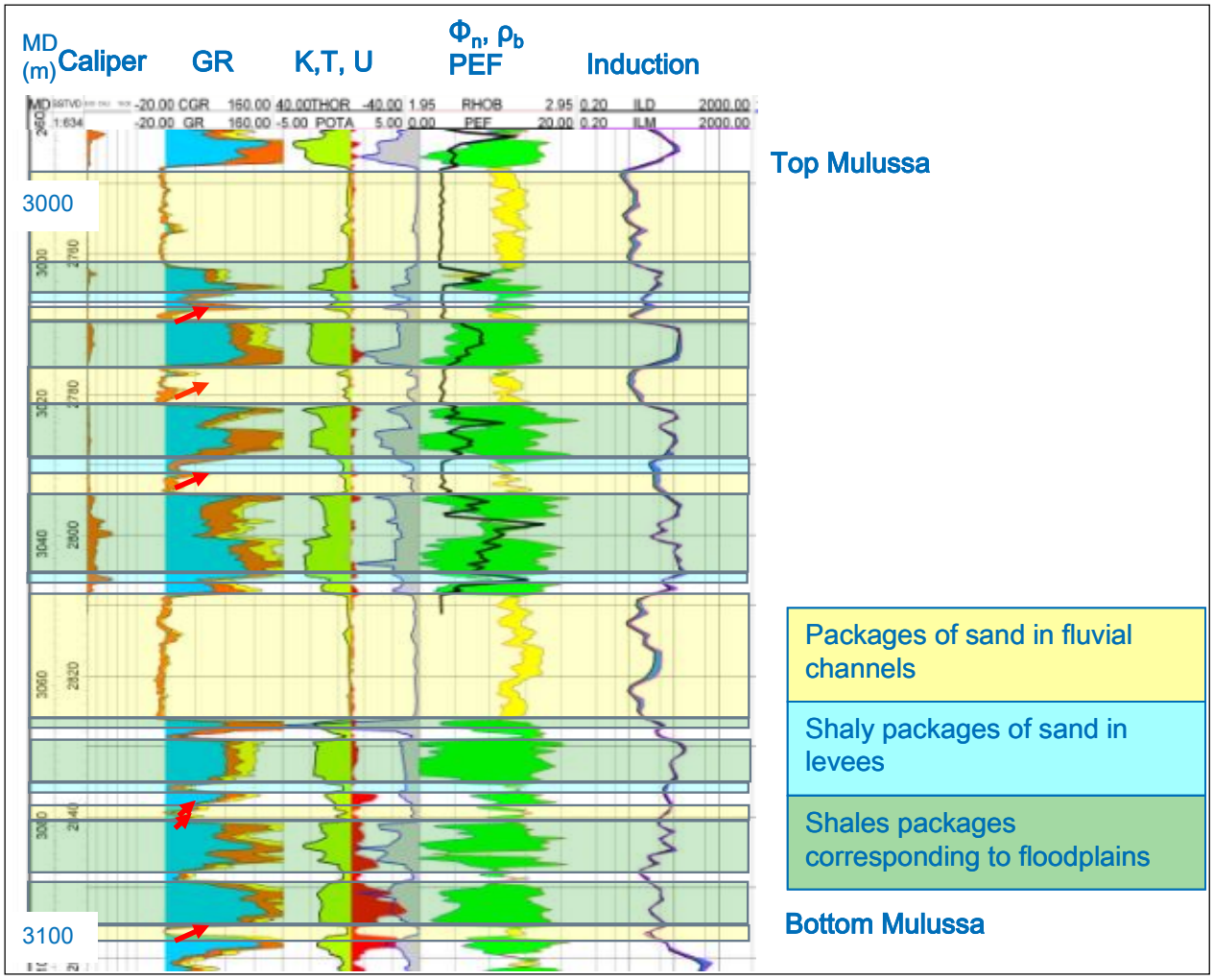

Figure 3.11: Interpretation of Mulussa F clasticFormation from 2011 students.

Rutbah Formation

In the 2011 project, the depositional environment of the lower Rutbah Formation resulted from the interpretation of core analysis and descriptions, core pictures and thin sections. In addition to this information, a quick look approach for log analysis, allowed them to determine two different environmental settings: 1) distributary channels (thinning-upwards sequence) and inter-channel environment (delta plain) and 2) distributary mouth bar features (coarsening upward sequences and trough cross bedding), which is in a more distal position.

Subsequently, the log analysis and the core interpretation were integrated in order to determine the three facies in the lower Rutbah Formation as well as the Mulussa F clastic Formation. The students used the GR log and divided it by three cut offs that showed a relationship between the environment of deposition previously found and the facies. The values used are presented in table 3.3 with the definition of the facies in each interval as shown in Figure 3.12.

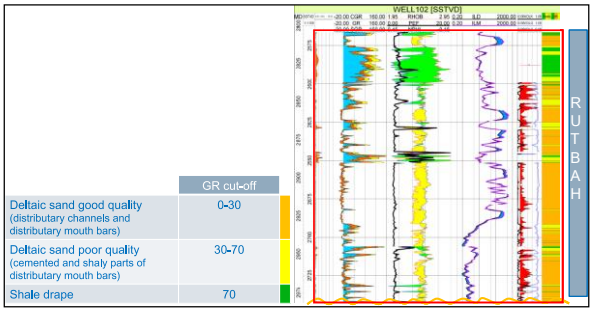

Table 3.3: The values used in the cut off and definition of the electrofacies. (From 2011 students)

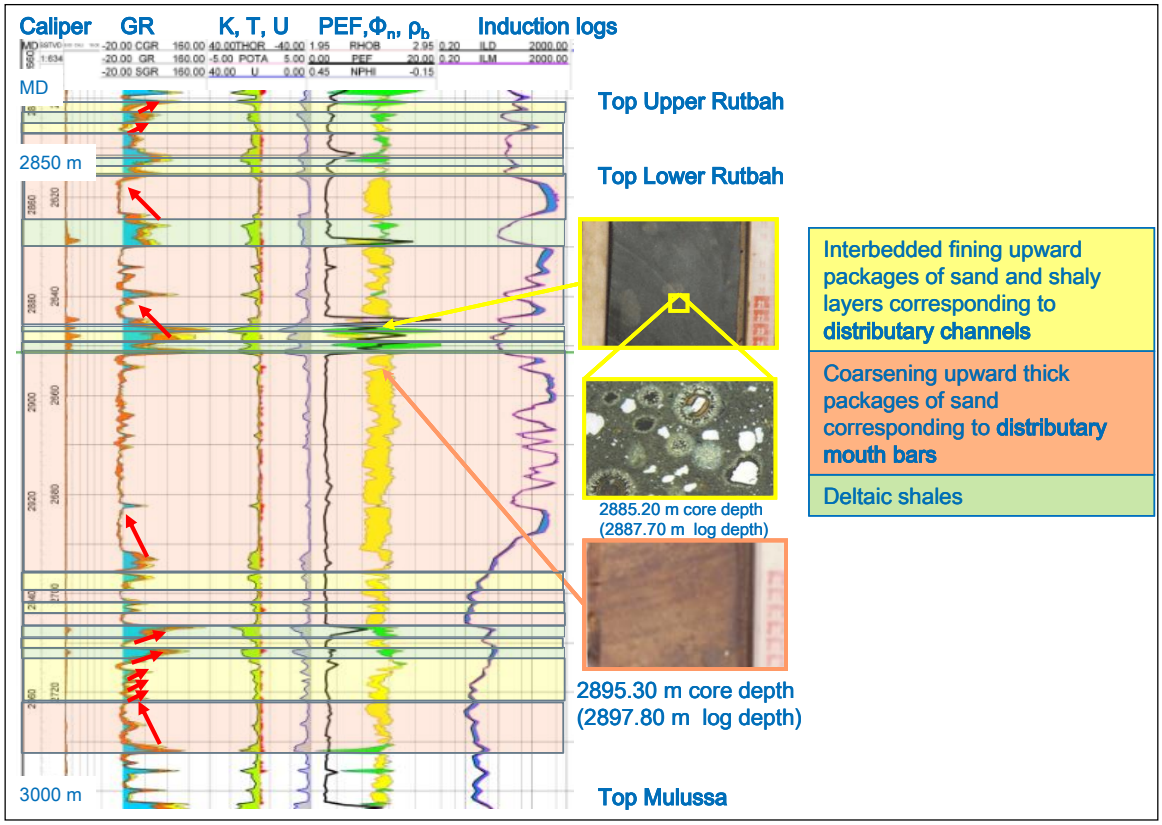

Figure 3.12: Interpretation of the Lower Rutbah Formation from 2011 students.

3.2.3 Improvements to be made

The fluid flow units of the reservoir model are defined by the sequences of facies identified in each formation. In the core description, we can distinguish more facies than the students defined in 2011 and subsequently more electrofacies from logs. For this reason, I proposed some improvements and these are shown in Table 3.4 with more details in the text below.

Environment of deposit	N/A	Good	Acceptable	To be refined
Rutbah			X	X
Mulussa F	X			
Electrofacies				
Rutbah			X	X
Mulussa F			X	X
Paleogeography				
Rutbah				X
Mulussa F				X

Table 3.4: Summary of the QC performed and decision of the improvements to be made

A new interpretation was created on paper using the description of the main sedimentary structures of the core, the pictures of the core and the GR log. They were then incorporated in Easytrace, together with a log recording grain size in the core to define the relationship between the vertical facies succession and the grain size.

The vertical succession of facies was interpreted as prograding –retrograding sequences on the core description (well 102). Then, in Easytrace software a new cut-off definition was used to relate the GR measurements to the shaliness. After validation on the cored well the cut-off computation was applied to the other wells of the database.

In order to understand how the sedimentary system evolved laterally from well to well in the area, it was necessary to interpret the paleogeographic configuration during the depositional time of each formation. Although the literature on this specific area was very limited, we built a model that integrates regional geology and the local information from ell data. See in the results.

3.2.4 Revised Interpretation

The results of the new interpretation of facies, facies association, relationship between facies association and grain size and also the definition of the environment are presented in the section of results, as well as the electrofacies and the definition of the paleogeographic configuration for each formation.

3.3 Stratigraphic Model

3.3.1 Dataset

Lower Rutbah Formation

Time-lines have been identified from the sedimentary model and the vertical succession of sequences at the wells. These lines must be correlated from well to well to delimit the spatial extend of the main sequences across the reservoir.

They are called stratigraphic units and represent the framework of the layering of the geological model. These units will also be used to define flow-units of the dynamic reservoir model

Mulussa F clastic Formation

For the Mulussa F clastic in the available dataset a thickness-width diagram of fluvial and distributary channels was given and used to define the extension of the sandy bodies.

3.3.2 Quality check of 2011 model

The students found a Mulussa F dolomitic as a marker to correlate the main units across the reservoir. They interpreted erosion of the dolomitic Derro Formation and then identified four large sequences in the Lower Rutbah Formation and five sequences in the Mulussa F clastic Formation. Figure 3. 13.

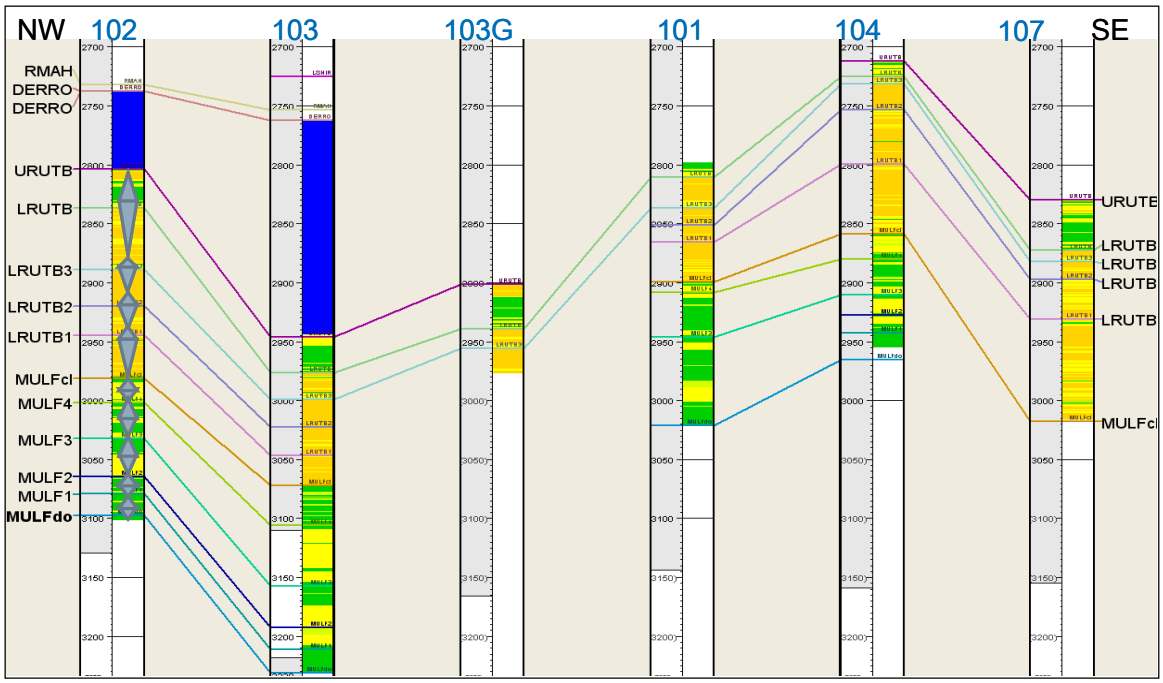

Figure 3.13: Correlation of the wells in structural position and definitions of the stratigraphic units.

3.3.3 Improvements to be made

Well to well correlation is observed in Figure 3.12. As seen on this figure, the students correlated the timelines of maximum flooding surfaces (MFS) for Mulussa F clastic formation, and the timelines of sequences boundaries (SB) for Lower Rutbah formation defining 9 flow units in total for both formations. As I defined different facies which are the main input in the model, I had to correlate me previous results and create a new model. Table 3.5 summarizes the changes made.

Time lines	N/A	Good	Acceptable	To be refined
Rutbah Mulussa F				X X
Main stratigraphic units				
Rutbah Mulussa F				X X

Table 3.5: Summary of the QC performed and decision of the improvements to be made

3.3.4 Revised Interpretation

We received in 2013 more information from the Operator Company of the FC field about the time lines and top markers defined in each well, so I refined these markers

with me own interpretation and created a new correlation based on the main MFS of the sequences. See in the results.

3.4 Static reservoir model

3.4.1 Dataset

The static reservoir model is the conjunction of all the models created before. It also integrates production data available at the initial stage of the reservoir, before production which correspond to: static pressure measurements (RFT and PVT data). In this part, the grid, zones and layers were defined, and the model was filled with the following properties: facies, porosity and permeability.

3.4.2 Quality check of 2011 model

In the 2011 project, the students integrated all the data acquired during the previous stages and built the model with 9 flow units. The thickness of the reservoir was divided into 59 layers plus one in the Derro Formation in a first approach which was considered a case of long term development.

In this model of 59 layers, 34 correspond to the Rutbah Formation and 25 to Mulussa F clastic Formation, with cell dimensions of: 100*100*7m(min=4m, max=20m in vertical dimensions) and a total of 370,000 cells. Table 3.6, (Figure 3.14)

Formation	Number of zones	Number of layers	Minimum	Maximum	Total Cells
Rutbah	4	34	4	20	
Mulussa Fdo	5	25	4	20	37000

Table 3.6: zones on 2011 model

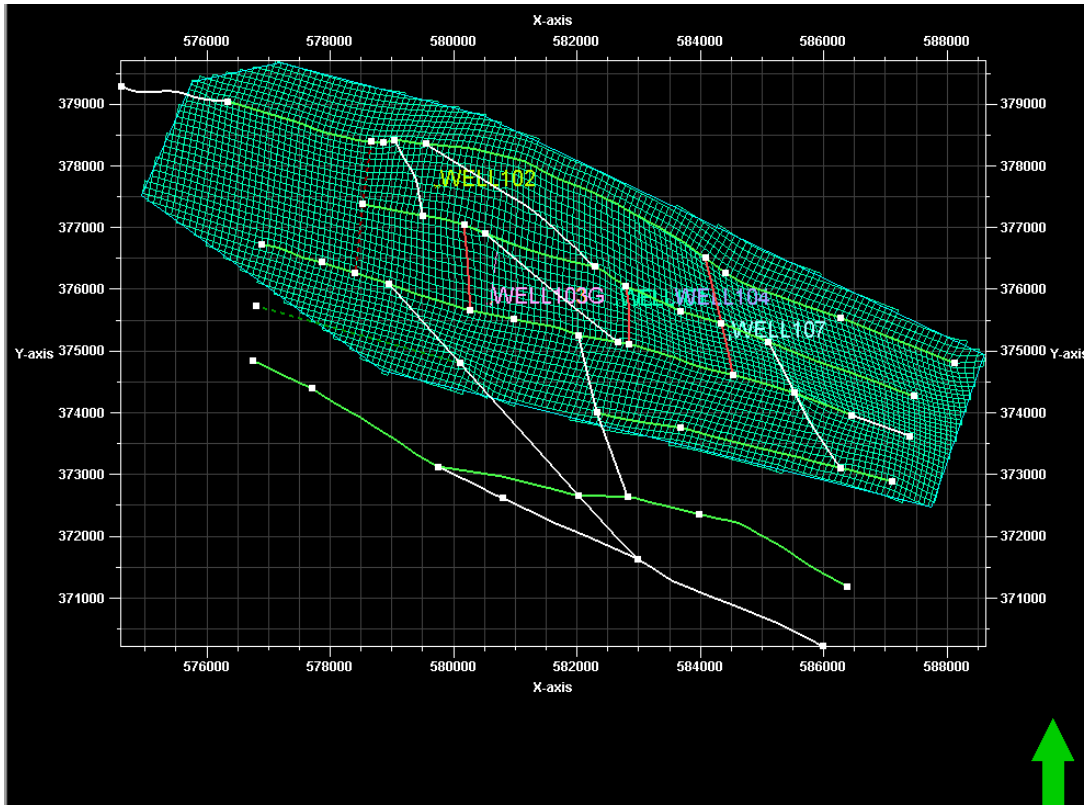

Figure 3.14: Definition of layering and gridding in the 2011 model.

In the 2011 project, for each flow unit the facies were defined using well data and blocked well data statistics. Two different algorithms were used depending on the depositional environment and the geometry of sand bodies.

For Lower Rutbah Fm. was used Pixel_based geostatical approach, using probability curves.

For Mulussa F clastic Fm, object based on approach, using thickness-width and the wavelength of channels and levees from the extrapolation made on the thickness–width diagram to the geological cross plot. (Figure 3.15)

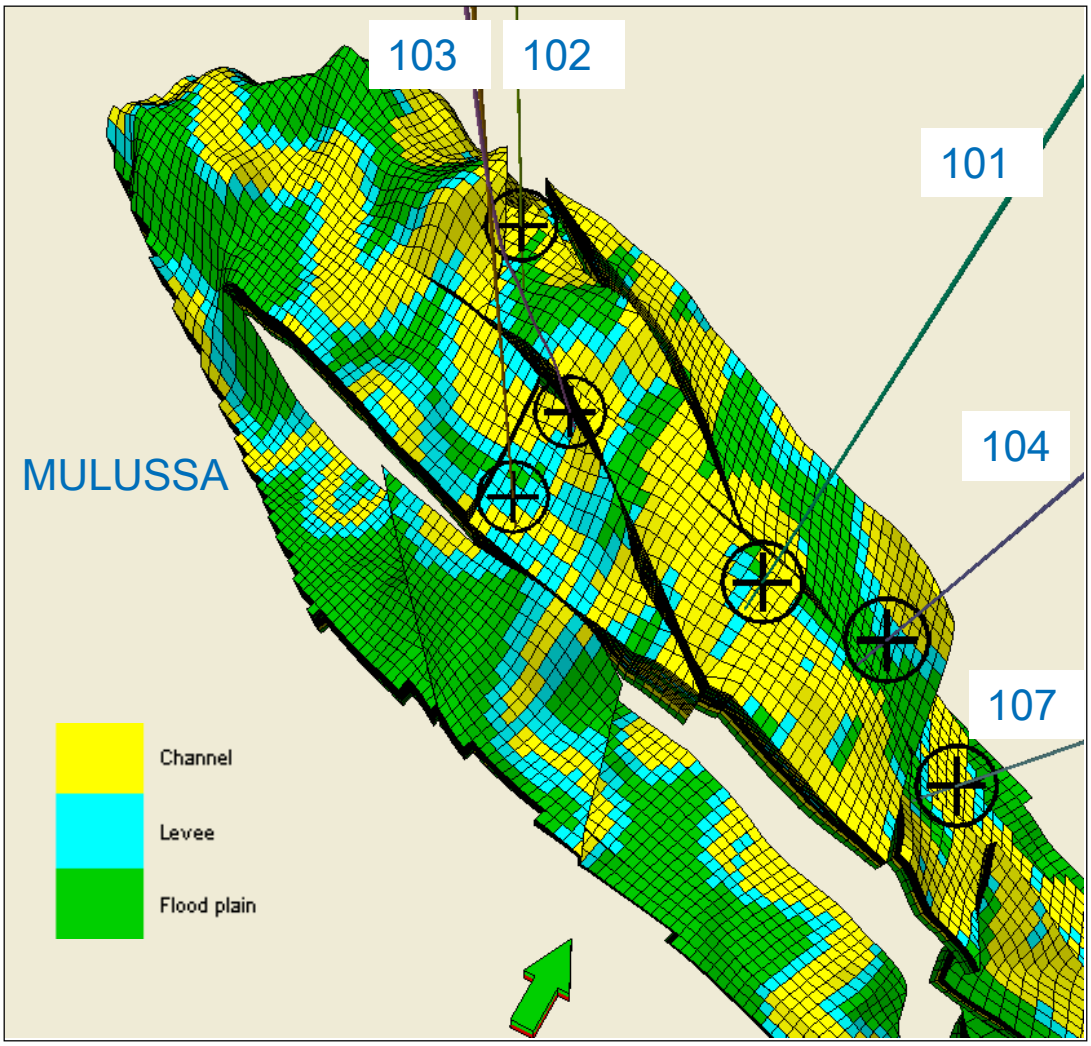

Figure 3.15: Final static model for the Mulussa F clastic Fm in 2011.

3.4.3 Improvements to be made

As mentioned previously, this part takes into account all the models defined in the previous stages. For this reason, the final model is the result of a multi-approach. Interpretation. In addition, as the model will be used in a training course, we considered that the model could be improved in regarding to the size of the cells and the number of layers in each formation. This is in order to decrease the time taken to run model and to avoid up-scaling for the dynamic part, since time is limited on the course. (Table 3.7)

Layerin-Grid definition	N/A	Good	Acceptable	To be refined
Rutbah	X			X
Mulussa F	X			X
Distribution of Properties				
Rutbah	X			X
Mulussa F	X			X

Table 3.7: Summary of the QC performed and decision of the improvements to be made

3.4.4 Revised Interpretation

The final model is presented in the results section. The Petrel software was used for the structural gridding and the property modelling. We performed 7 main flow units, three in the Mulussa F clastic and 4 in the Rutbah. As for the 2011 model, a pixel_based approach was used for the Rutbah Formation and a object based_approach was used for the Mulussa F clastic. Formation.

Information from the relationship between thickness and width given by the company, as an input when modelling the Mulussa F clastic Formation.

During this stage, continuous controls of the results was necessary, in order to check that statistics from logs, blocked logs and model were consistent. Moreover it was necessary to carry out visual quality control in the Mulussa F calstic fm. as object modelling might give non-geological features.

4. RESULTS

The results presented in this chapter are divided into four sections: the structural model, the sedimentological model, the stratigraphic model and the static reservoir model.

4.1 Structural model

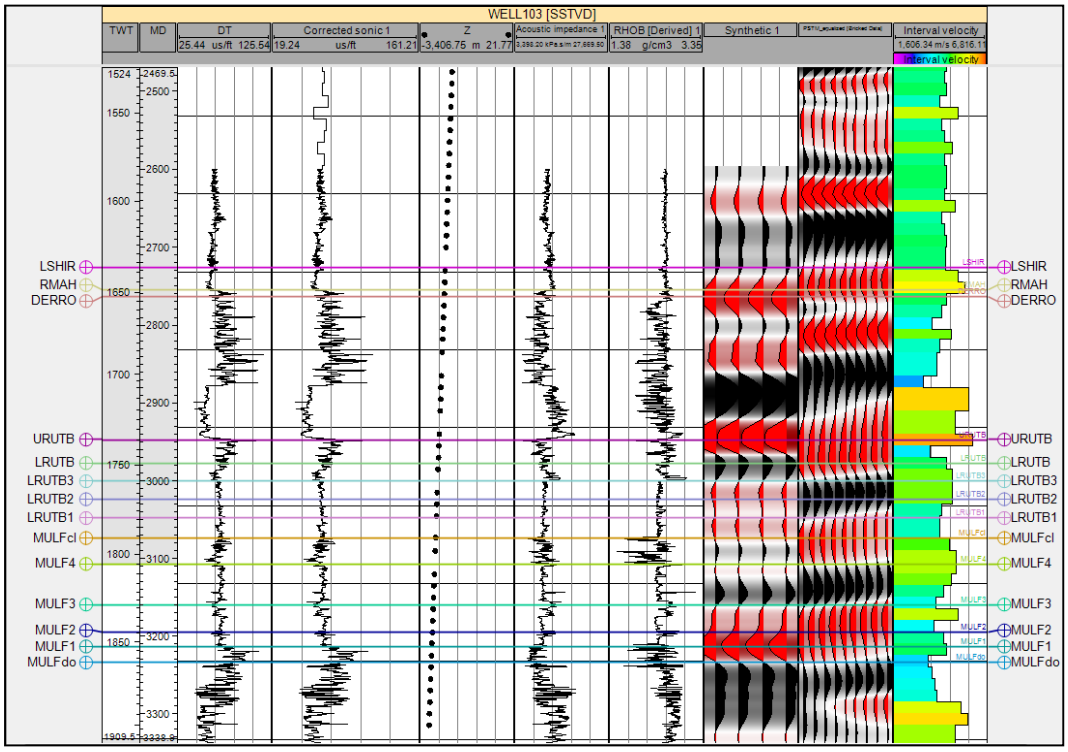

Figure 4.1 Synthetic seismogram of well 103, using a Ricker wavelength (frequency 30 hz)

A new synthetic seismogram of well 103 was created, in order to perform an accurate lithologic calibration of the seismic stratigraphy and to interpret the horizons (table 4.1)cross the seismic cube. See Figure 4.1.

Formations	Horizons TWT	Surfaces TWT	Surfaces Depth
Top Derro	Derro	Derro	Derro
Top Upper Rutbah	Upper_Rutbah	Upper Rutbah	Upper Rutbah
Top Mulussa Fdo	Mulussa F dolomitic	Mulussa F dolo	Lower Rutbah
			Mulussa F clas
			Mulussa F dolo
Paleozoic	Paleozoic	Paleozioc	Paleozoic

Table 4.1:Horizon and surfaces used in the 2013 model

4.1.1 Faults model

Due to the complex structural setting of the area, the extraction of the amplitude on the Paleozoic surface led to a good definition of the lateral extent of the faults. In the interpretation, I defined three main normal fault trends: NW-SE, SW-NE and NNW-SSE. The SW-NE trend appears to cut the NW-SE trend, although in other segments the opposite case is observed. (Figure 4.2 and 4.3) It could be related to a reactivation of the pre-existing extensional setting or to a conjugate system by the geometric relationship between the fault trends. See in discussion.

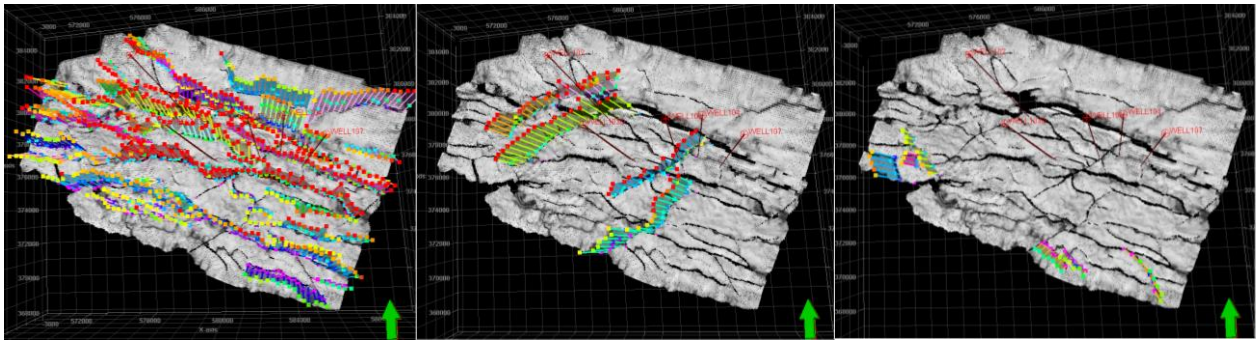

Figure 4.2: Fault trends identified a: NW-SE; b: SW-NE c: NNW-SSE.

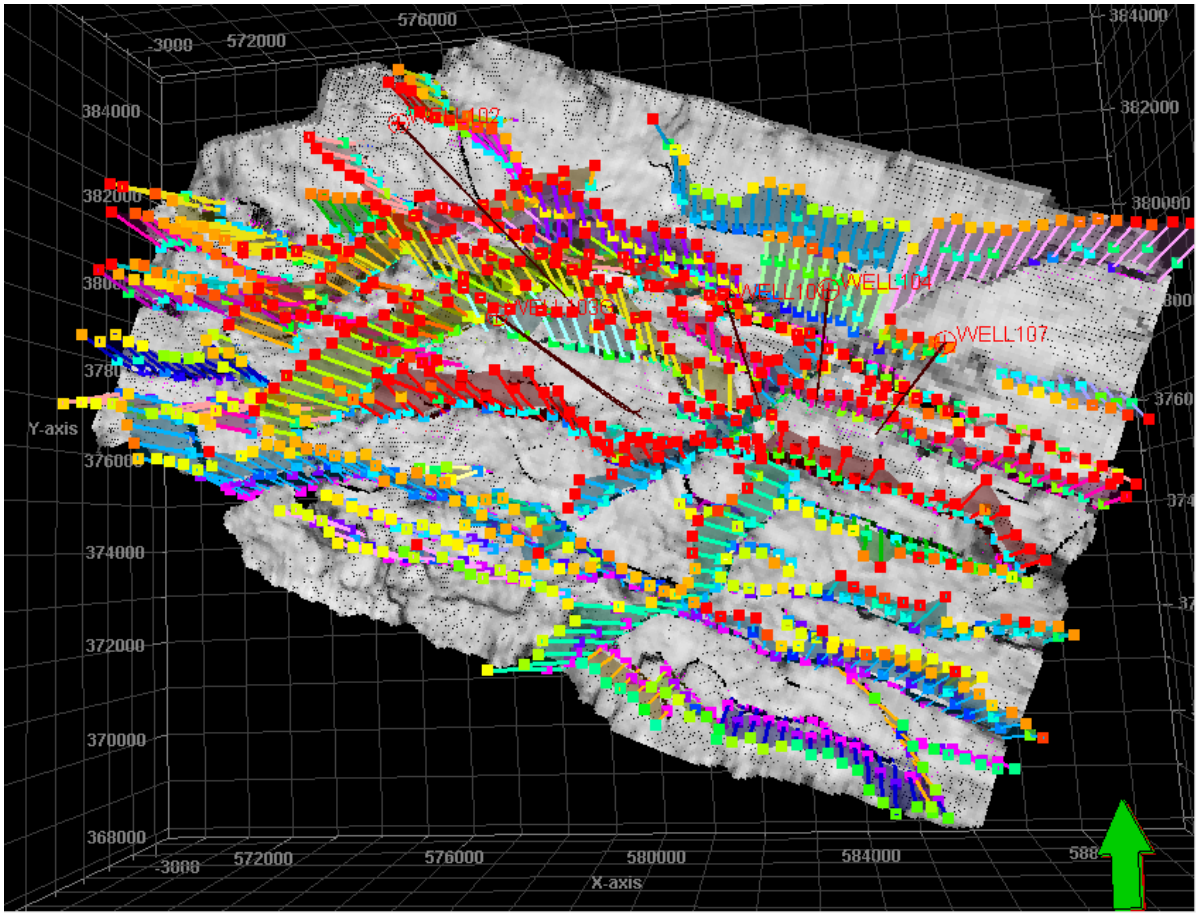

Figure 4.3: Global view of the identified faults trends

In the area of study, the geological context corresponded to an extensional setting in the Coniacian, associated with the formation of the Euphrates Graben. Afterwards, distension occured in the Turonian, followed by the reactivation of normal faults Inversion is known from the Miocene to present (Brew, 2001).

However, in this interpretation, all faults presented the characteristics of normal faults and no inversion of the system was recognized. The fault throw of the main normal faults of the study area was calculated around 400m.

The fault throw determine the role that the fault plays in terms of being a connecting fault (reservoir – reservoir) or a disconnecting fault (reservoir – seal or non-reservoir layer). In the area of study, based on seismic interpretation and pressure data from wells, most of the faults are considered as disconnecting faults. As a result,

in the field I took this information into account to preserve the non-connectivity of isolated blocks. See Figure 4.4 and 4.5.

In total 51 faults were interpreted and divided into three fault families: 40 NW-SE trending faults, 5 trending SW-NE and 6 trending NNW-SSE. Since the free water level (FWL) delimits the production area within the field, not all of the faults were used in the structural model.

Furthermore, the short length faults and those that are not connected to the reservoir fault network were omitted in order to simplify the model. Thus, only 20 faults were used to build the model, 16 from our own interpretation and 4 from the previous model data. These four faults were not picked on the seismic data but were added to compartmentalize the reservoir, as observed on the production data. Figure 4.4. The structural model was built in the depth domain. Figure 4.5

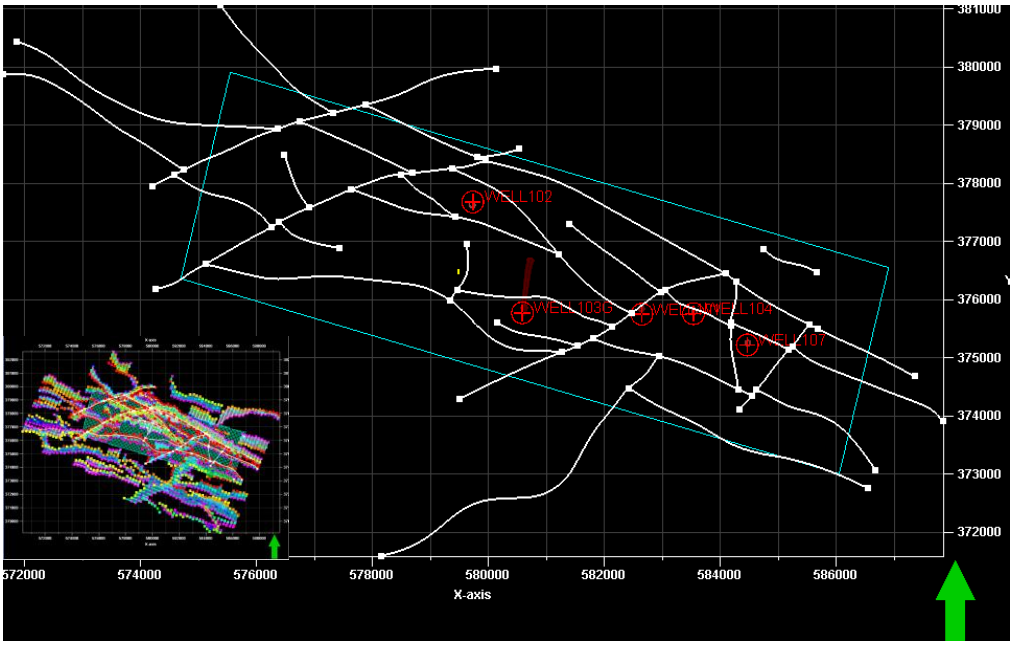

Figure 4.4: Top 2D view of the structural model

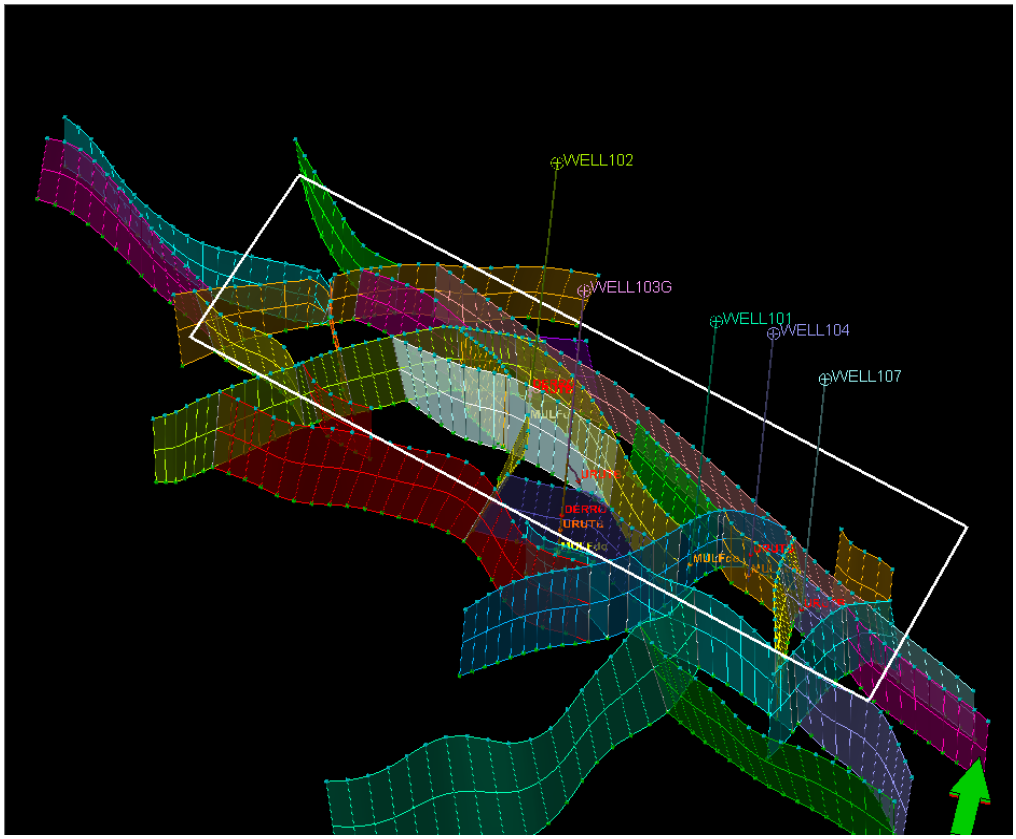

Figure 4.5: 3D view of the fault model, in depth

4.1.2 Surfaces (in time and depth domains)

The main traps identified in the area of study correspond to faulted blocks, tilted blocks and horsts, with internal panels in the N120/N160/N40 directions associated with the Euphrates Graben structure. Faulted blocks can be identified on the maps of Paleozoic, Mulussa F dolomitic and Rutbah formations where the FC field is located. The fault throws decrease from the Paleozoic to the Upper Rutbah Fm.(Figure 4.6). The FC field is divided by faults into two minor blocks: 1) block including wells 103 and 102 and 2) wells 101, 104 and 107.

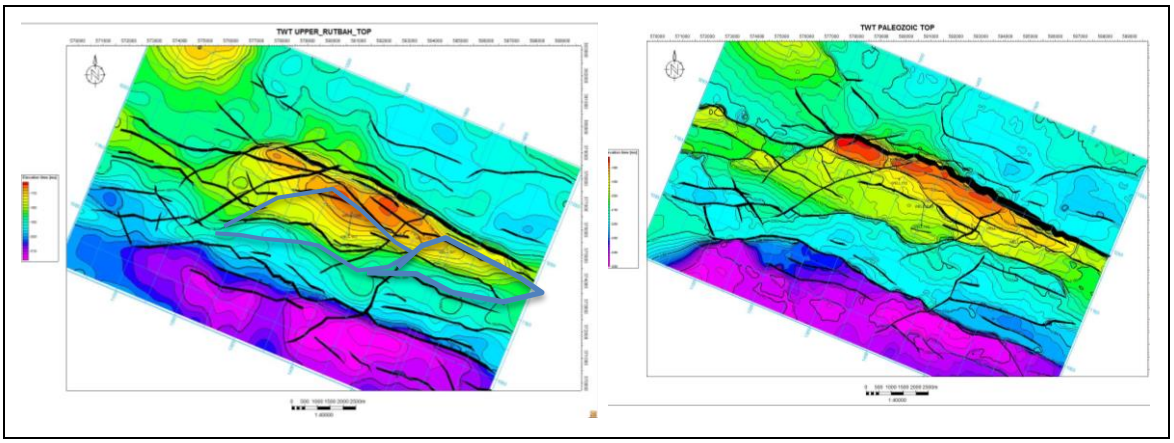

Figure 4.6: TWT Maps of Top Upper Rutbah including two minor blocks (left) and Top Paleozoic (right)

The deepest area is located in the southwestern part and the highest zone is situated in the center of the area, which also corresponds to the FC field. In general, the units interpreted have a good continuity in the seismic cube.

As these surfaces are an input for the construction of the static geological model, I had to create the surfaces of the Top Mulussa F clastic Fm and of the Top Lower Rutbah, Fm which correspond to the tops of the two reservoirs of the field. Although it was not possible to follow these horizons on the seismic cube, they were identified as markers in 5 wells. These surfaces were then created by interpolation between the under and overlying surfaces interpreted from seismic, and the well markers (Figure 4.7). This process could be a source of uncertainties in the static modeling workflow (see the discussion part).

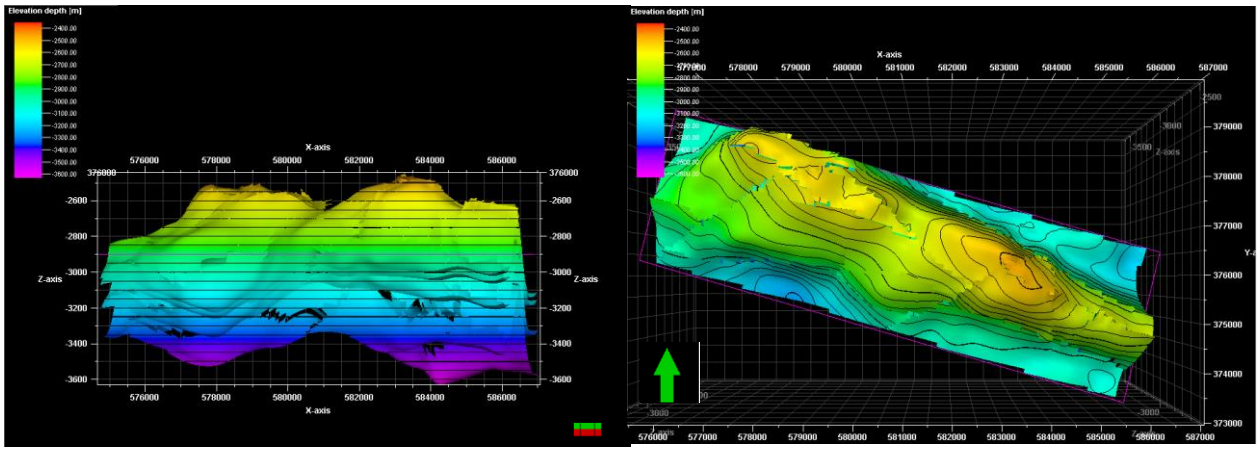

Figure: 4.7 Structural model in depth including Lower Rutbah and Mulussa F clastic Formations

4.2 Sedimentological model

Rutbah Formation

All facies associations are described in table 4.2 and Figure 4.8, with more details in the text. The depositional environment of the Rutbah Formation is related to a deltaic system.

In the core of well 102, the patterns of the facies successions allowed me to distinguish between retrograding and prograding sequences within this deltaic environment. In this analysis, I determined 6 facies associations. Some of the facies associations presented similar qualities in terms of reservoir and also had similar characteristics, so these were put together and subsequently only 5 remained for the master log. The facies associations are described from high to poor quality for a reservoir (Figure 4.8). A schematic diagram of the facies associations found in the core of the Rutbah Formation in Table 4.2

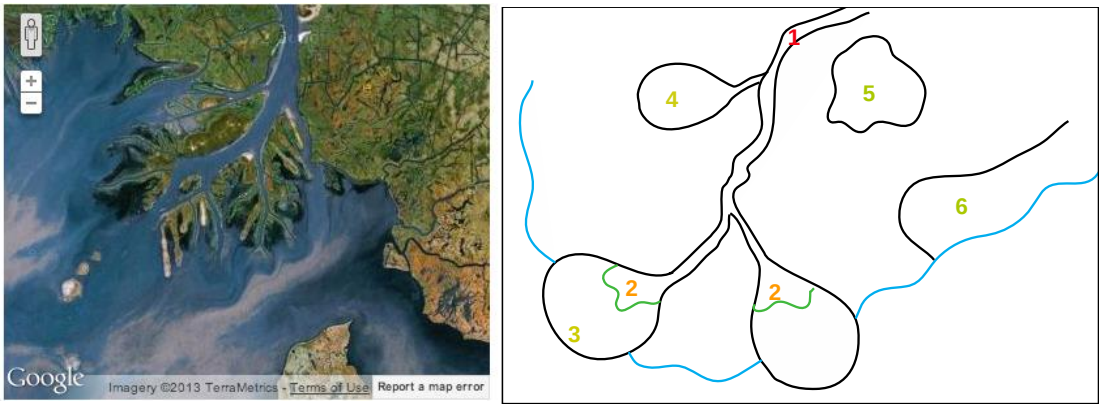

Figure 4.8: Schematic diagram of the deposit environment in Rutbah Formation. The numbers of the figure correspond to the numbers in the table 4.2.

	Facies from well 102					
Facies Association	1	2	3	4	5	6
1	DC					
2		PMB				
3			DMB	CS		
4					CP	B

DC	Distributary channels
PMB	Proximal Mouth Bar
DMB	Distal Mouth Bar
CR	Crevasse splays
CP	Coastal Plain
B	Bay

Table 4.2: Facies associations in well 102 in the Rutbah Formation.

The facies association with clean sandstone showing a fining upward grain size evolution from coarse to fine and sedimentary structures of trough cross-bedding and current ripples (representing an unidirectional current) were related to major distributary delta channels. In addition, this is the most predominant facies association in the well and it can be 3 to 10 meters thick. This thickness could suggest a high sedimentation rate.

These sequences are generally eroded by the channel bed of the new system. This is interpreted as a consequence of the lateral migration of the system (new channels migrate and erode the finer sediments of the previous one). This process could have led to the stacking of the sand-bodies, improving the thickness of the reservoir within the basin. In Figure 4.9 the distributary delta channels is represented with red.

The crevasse splay deposits were identified by sequences of shaly sandstones which were often cemented. This facies association is not very common in the Rutbah Formation section. The thickness of crevasse splays ranges from one meter to a few centimetres. It generally appears overlaying distributary channels, because it is produced when the distributary channel stream breaks levees and begins to deposit sediment on the deltaic plain. For this reason the sediments deposited do no form clean sandstone.

Although the crevasse splay deposited is linked to areas closer to coastline than distal mouth bars, it presents poor reservoir characteristics. Crevasse splay is discussed in this section because the environment of deposition is more related to the processes of the distributary channels than the proximal mouth bars. In the Figure 4,9 it is indicated by yellow, and in Figure 4.8 it corresponds to number 4.

The next facies association corresponds to mostly medium-grained clean sandstone with some intercalation of thin layers of coarse-grained of less than one-meter sandstone. Thus no trend was identified. Regarding sedimentary structures: this facies association presents low angle bedding (indicating the aggradation of the

system). This facies association was related to proximal mouth bars and is more frequent on the middle part of the formation. However, I do not have the core of all the lower Rutbah Formation in order to determine its frequency. See details in Figure 4.9 where the facies association is shown in orange.

Moving toward deeper environment, there are distal mouth bars which present similar features to those I identified in the crevasse splay sequence. The facies association of the distal mouth bar corresponds to shaly sandstones, often cemented with alternation of a few milimetres of argillaceous layers; this could be related to tidal influence in the system.

This depositional setting is more common in the upper part of the Lower Rutbah with a thickness of up to 10 meters. Low energy and fine sediments could suggest more distal unit. In Figure 4.9 this is represented by light green.

The more shaly units found in the core correspond to coastal plain or bay fine sediments, with bioturbated shales which are sometimes cemented, which could create heterogeneities in the reservoir. The thickness of these sequences is between 5 and 10 meters in the upper part of the core.

To summarize, in the Rutbah Formation the main reservoir is the Lower Rutbah because the Upper part corresponds mainly to shale. In addition, with the facies associations found in the core, it is clear that the environment of deposition was related to a deltaic system. In Figure 4.9 the grain size log created from the core data is shown in the fourth column and it is possible to recognize a relationship between the fining upwards grain size and the proximal facies associations (channel-fill sequences).

On the log, the coarse to medium grained sandstones are represented by red and orange. However, this grain size range can either correspond to proximal mouth bar or crevasse splay. These two facies associations cannot be distinguished by the grain size criteria only.

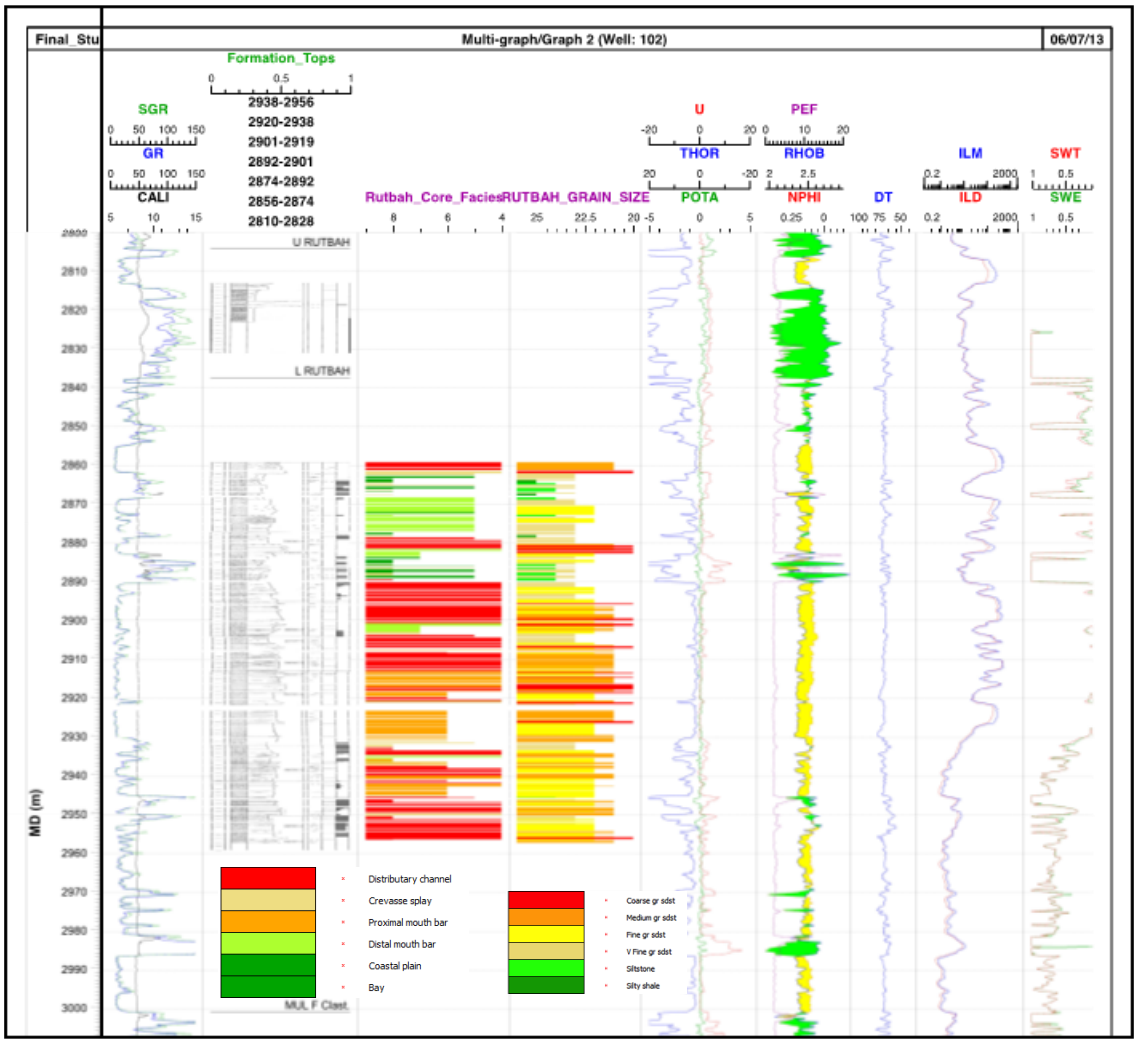

Figure 4.9: Facies association and grain size. Column 3 correspond to core facies and column 4 to grain size.

Mulussa F clastic Formation

In the dataset received for the Field Challenge 2011, 3 facies associations were given: channel, levee and floodplain corresponding to a fluvial system. The sedimentary environment has been interpreted as an anastomosing fluvial system which (Figure 4.10), by definition, corresponds to multiple, interconnected, coexisting channel belts on an alluvial plain. This type of river system most often forms under relatively low-energy conditions near a local base level. (Masaske, 2000).

Such channels display a very blocky shape on the gamma-ray log (SGR log on Figure 4.9) which helps to interpret subsurface data.

Figure 4.10: Showing an anastomosing fluvial system, environment of deposition of Mulussa F clastic Formation

In the determination of Electrofacies, I used different cut-offs for each formation (see table 4.3). The values used in SGR log gave me an estimation of the shaliness of the formation. Due to the way SGR log measures the natural gamma radiation emanating from a formation (split into contribution from each of the major radio-isotopic sources Th, U, K (Glover, 2001)), the values of these isotopes increase in the shales, thus the low values correspond to clean sandstones (Table 4.3).

SGR Log cut off	Rutbah Formation
0-10	Very clean sdst
10-15	Clean sdst
15-35	Siltstone
35-50	Silty shale
>50	Shale

SGR Log cut off	MulussaF Formation
0-32	Very clean sdst
32-50	Clean sdst
50-105	Silty shale
105-200	Shale
>200	Tuff

Table 4.3: Values used for the SGR log cut-off in each formation.

In the case of the Rutbah Fm, I was able to calibrate the values used for the cut-off with the core data and recognized the best values which matched it. On the other hand, for Mulussa F clastic Fm, the quality control of the values used corresponded to a comparison with the facies core data received. However, the highest values of

the SGR log were defined as tuff layers (Figure 4.11). After an accurate matching in well 102 these values were propagated to the others wells.

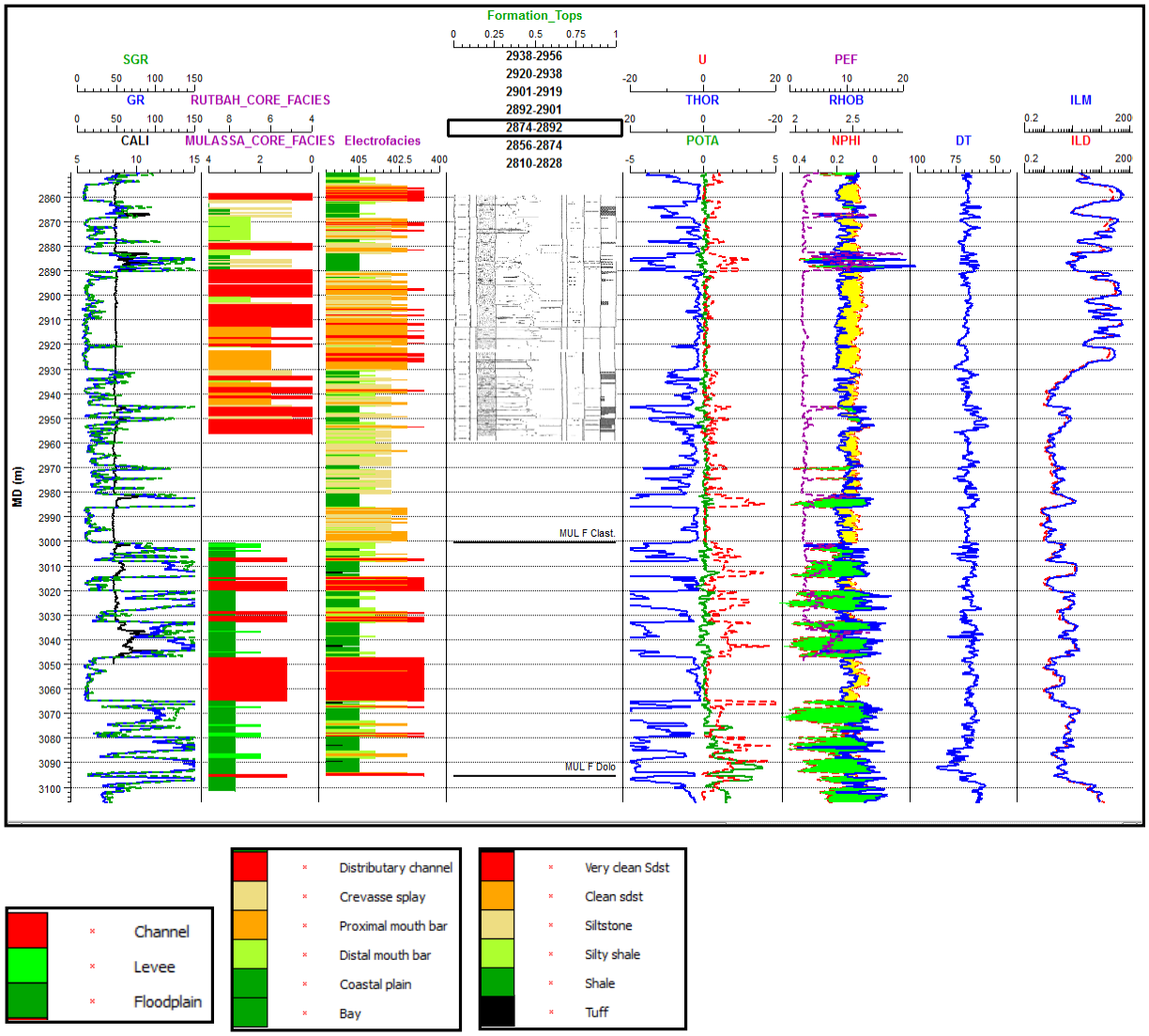

Figure 4.11: Masterlog with Electrofacies determined and the facies interpreted from core data.

Paleogeography of the Rutbah Formation

The paleo-direction of sediment transport should be identified to correlate the sequences and facies associations from well to well and then define the spatial extension of the reservoir.

This proximal-distal polarity is often given by the sedimentological interpretation and the regional topography at the time of deposition.

I have analysed the regional paleogeographic maps available (Brew, 2001) and deduced that the local source area for the deltaic system during the lower cretaceous was located in the southeast part of the field, which correspond to the Rutbah-Rawdah uplift. The coastline at this time was located in the northwest. This implies that the direction of the flow was from the southeast to the northwest. A pinch out of the sand-bodies as well as a degradation of the reservoir facies is then expected in this direction. In addition, some lateral variations are expected due to the deltaic system itself (Figure 4.12).

The location of the wells seems to be parallel to the source area so I expected similar configuration of the facies sequences in those. However, the deposition of these sequences could be affected by some paleo-highs, reducing the space of accommodation for sedimentation and thinning the sequences.

Figure 4.12: Paleogeographic of the Rutbah Fm.

Paleogeography of the Mulussa F clastic Formation

The deposition of the Mulussa F clastic Fm in the area of study corresponded to a fluvial system and more specifically to an anastomosing river environment. I interpreted, based on Jamal 2001, that the material supply came from the southeast and that the coastline was located to the northeast. In the wells there is a relevant thickness variation in well 103, which could be related to the subsidence in the basin during the upper Triassic which was also the responsible for the tuff layers observed in the sequence (See in discussion).

In the anastomosing rivers the sand bodies presented a greater elongation than in the meandering fluvial system. This could have implications on the reservoir properties.

4.3 Stratigraphic model

In the stratigraphic model, I used all the data created in the sedimentological part, a propagation of the SGR cut-offs defined over all the wells. I used the markers received from the company and checked with the sequences determined in the wells. Some of the MFS were moved to the peaks of the Thorium - Uranium logs which indicate the major shale breaks. Thus these markers represent the time lines of the maximum flooding surfaces in the basin as well as the major shaliness and were used in the correlation (Figure 4.13).

In the Rutbah Formation, 5 main MFS were recognized on the wells and were called (from bottom to top) MFS1, MFS2, MFS3, MFS4 and MFS5. However, only MFS1, MFS2, MFS3 and MFS5 are present in all the wells, so these four markers were correlated. MFS5 is in the Upper Rutbah and was used to flatten the correlation in order to define the geometry of the basin at this time (Figure 4.14). As a result wells 103 and 101 could be located in a high paleogeographic area during the deposition.

Meanwhile wells 102, 104, 107 seem to indicate a small paleo-depocenter. See in the discussion.

The main reservoir is in the Lower Rutbah Fm. Thus, 4 zones in the Lower Rutbah Fm were created and the subdivision inside was defined by the correlation of the sand-bodies well to well (Figure 4.15).

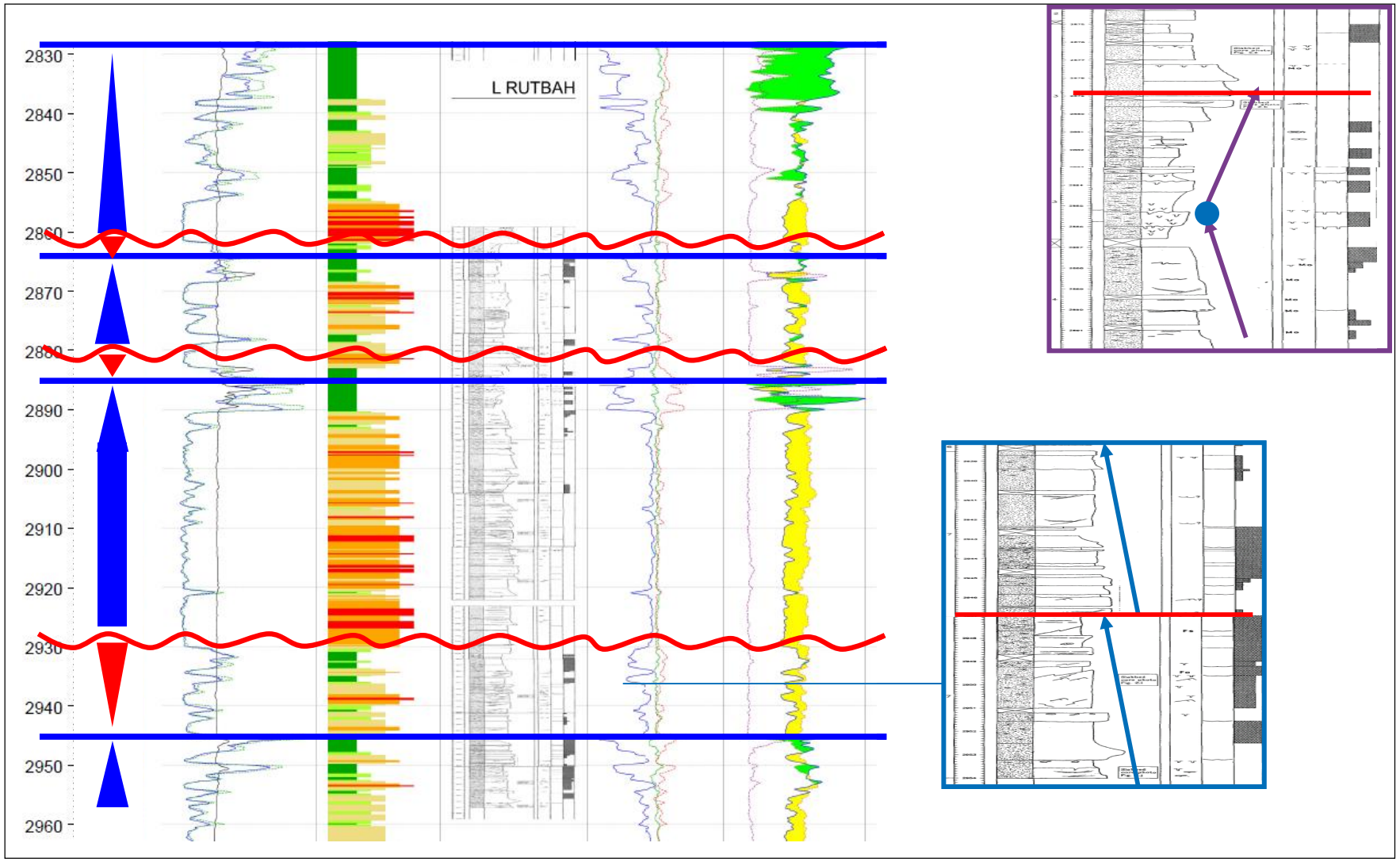

Figure 4.13 Definition of MFS in Rutbah

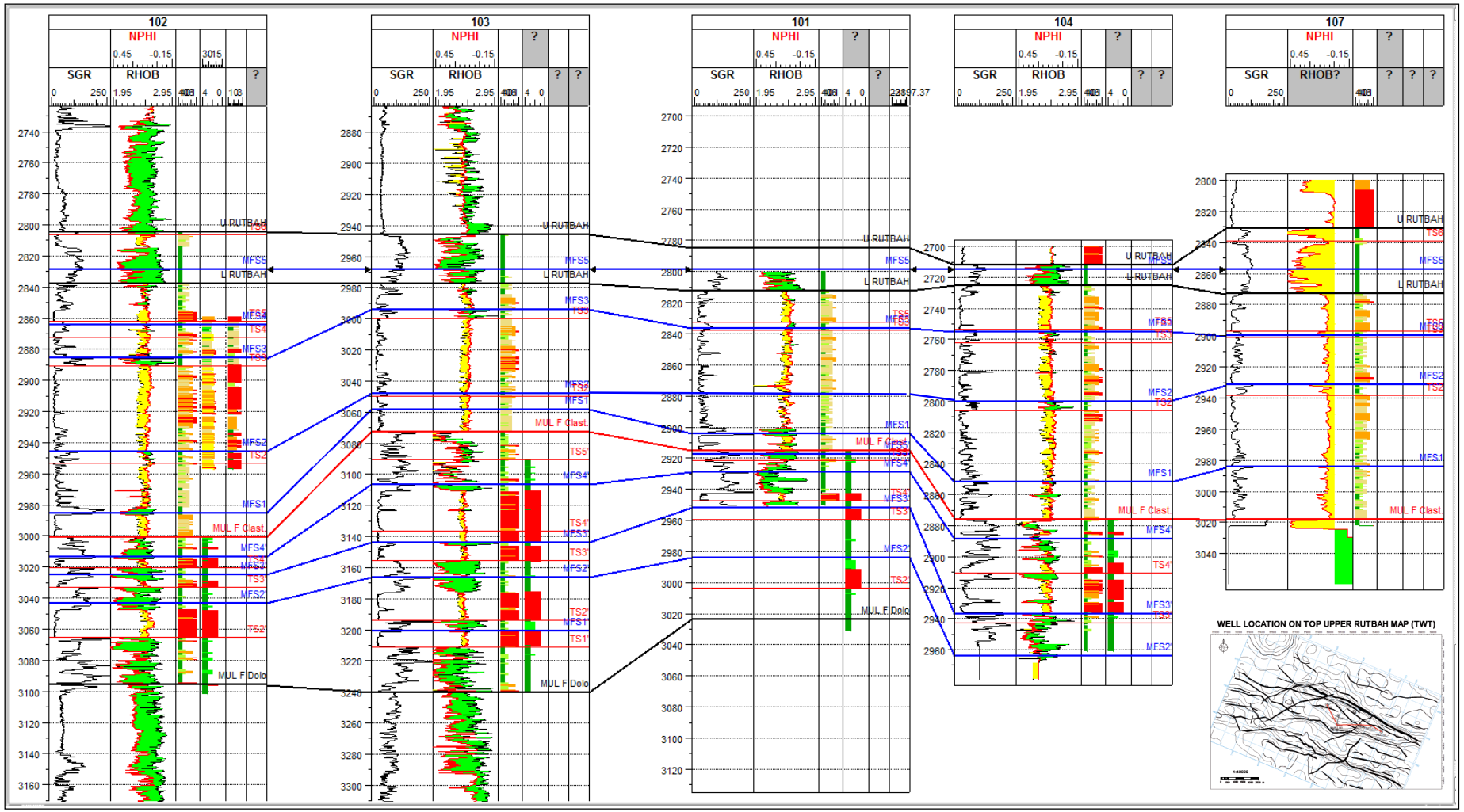

Figure 4.14: Well to well correlation of the MFS

In the case of the Mulussa F clastic Fm, 4 MFS were interpreted using the SGR log and named (from bottom to top) MFS1', MFS2', MFS3'and MFS4'. For the correlation only MFS2', MFS3' and MFS4' were used because these were present in all the wells where the Mulussa F clastic was drilled (Figure 4.13). These wells were 102, 103 and 101, they are located to the northwest of the field. On the correlation panel, well 103 presents a higher thickness than the others, which could be related to the subsidence at the time of deposition and be related to a local depocenter. In addition the sand-bodies correlations were done with respect to the width/height ratio of the channels, as given in the Field challenge dataset.

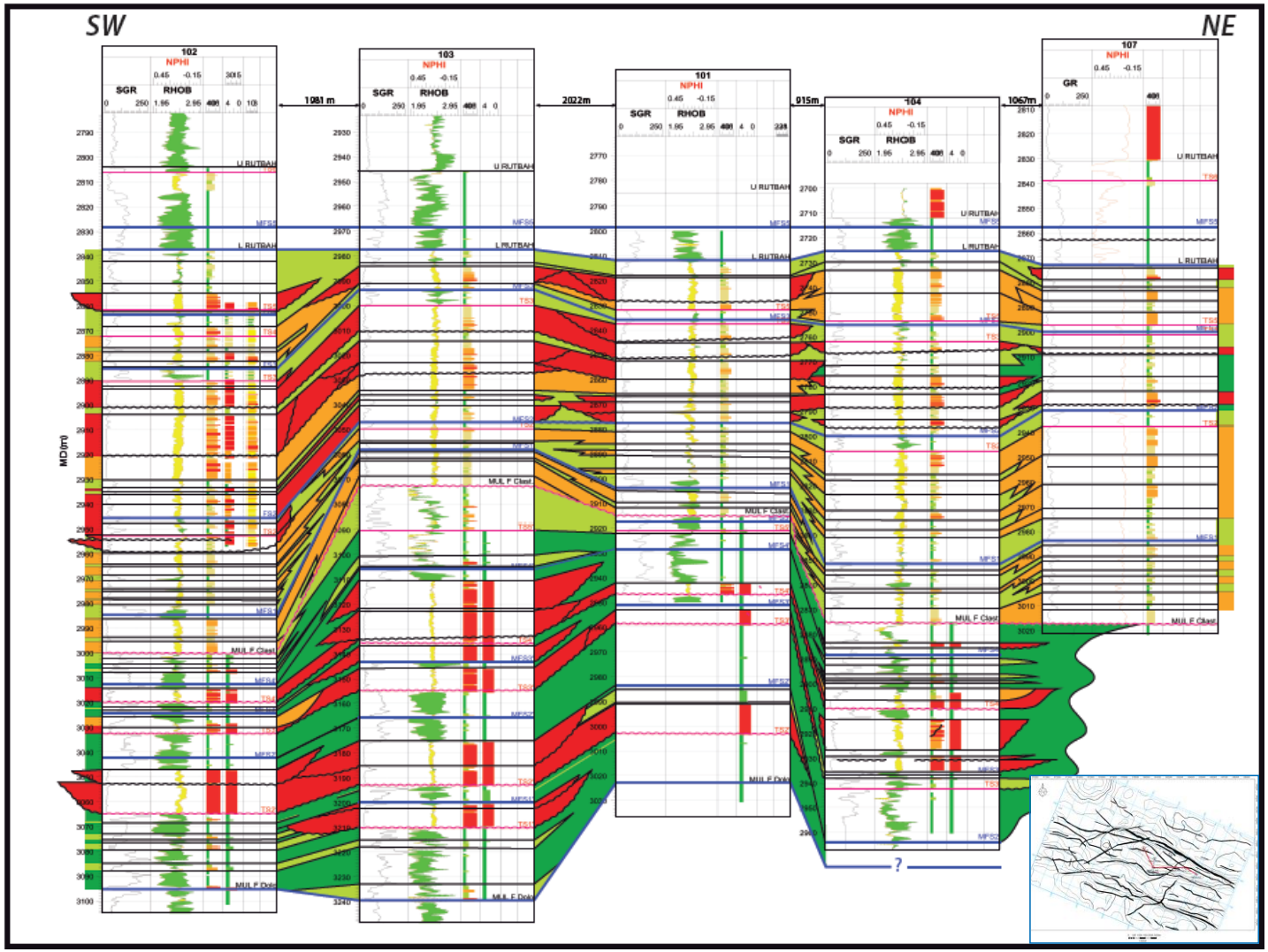

Figure 4.15: Correlation scheme showing the MFS (blue lines), the TS (straight red lines) and the erosions or unconformities (ondulating red lines) together with the main sand bodies.

4.4 Static Reservoir Model

In the static reservoir modelling task, the time-depth conversion was performed before the gridding. I used a framework of 20 faults, 5 horizons of Derro, Upper Rutbah, Lower Rutbah, Mulussa F clastic and Mulussa F dolomitic (Figure 4.16). In the gridding the size of the cell is 100m * 100m.

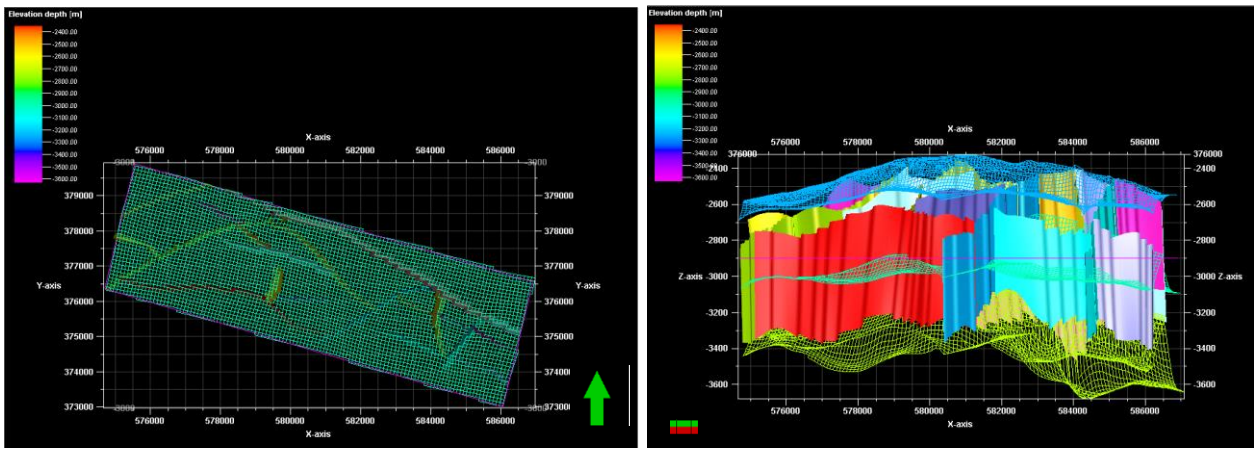

Figure 4.16: Gridding of the FC field in the 2013 reservoir model

For the Lower Rutbah Fm.4 zones were created based on the main 3 MFS and for Mulussa F clastic Fm. 3 zones were created based on 2 MFS. The definition of zones is shown in Table 4.4 and Figure 4.17. Subsequently, the internal structure of the zones is defined by the number, thickness and geometry of the layers. It depends on the stratigraphic system and the nature of the surface (correlative or erosive) at the top and at the bottom. (Figure 4.18). The average thickness in the proportional intervals in vertical layering correspond to 2 m (see details in Table 4.5).

Reservoir	Surface	Zone	Distribution Layers
Lower Rutbah	Lower Rutbah	Rutbah 4	Follow bottom
	MSF3	Rutbah 3	Proportional
	MSF3	Rutbah 2	Proportional
	MSF3	Rutbah 1	Follow top
Mulussa F. Clastic	Mul. cl	Mul. cl3	Follow base
	MSF4'	Mul. cl2	Proportional
	MSF3'	Mul. cl1	Follow top
	Mul. dol		

Table 4.4:Definition of the zones in 2013 reservoir model

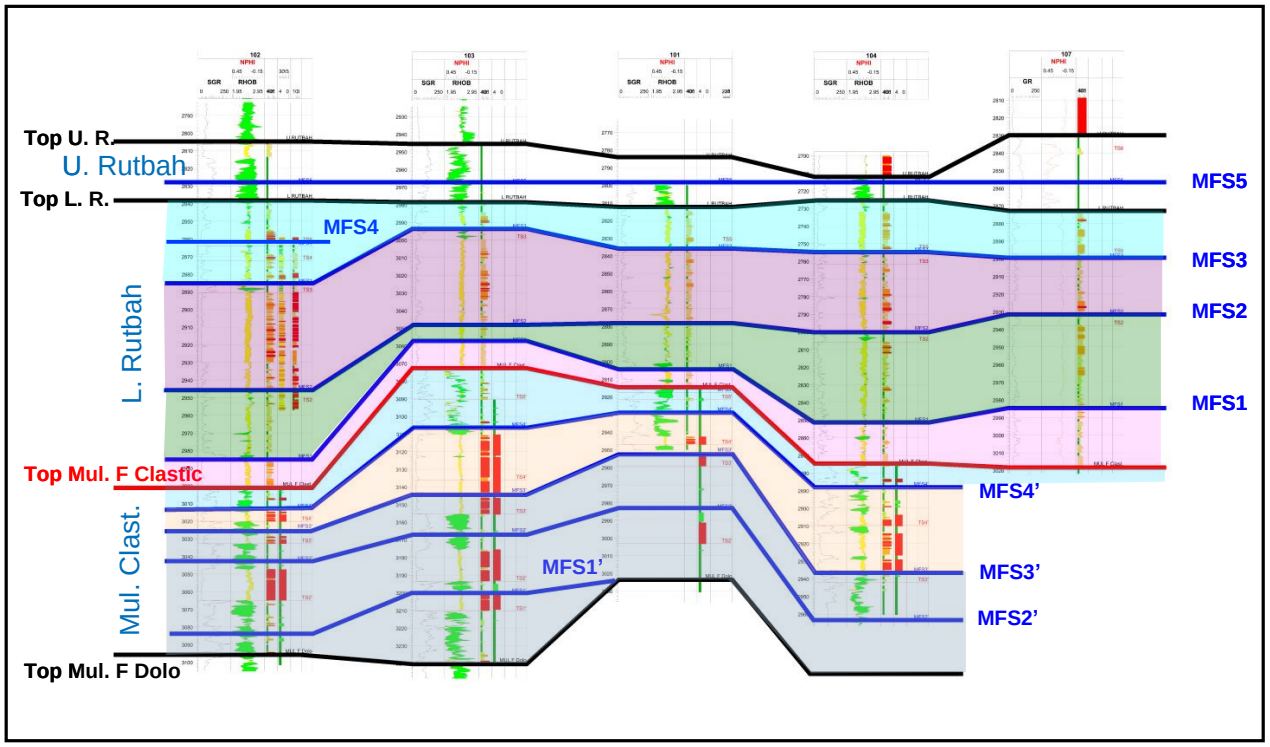

Figure 4.17: Definition of the zones based on MFS in the 2013 reservoir model.

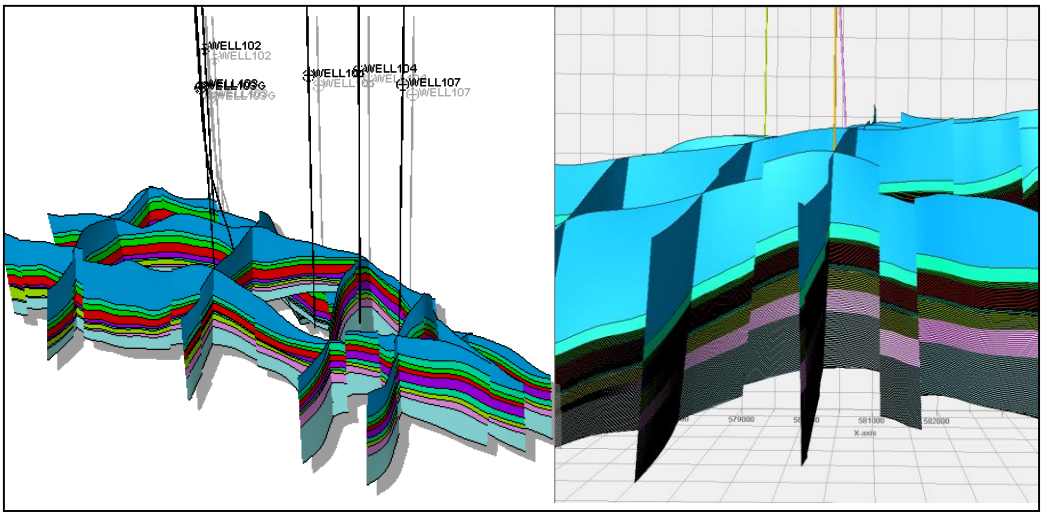

Figure 4.18: Zones and layers defined in 2013 model from Derro to Mulussa F dolomitic

Reservoir	Zones	Min	Max	Average	Numbers of Layers	Average layer Thickness
Lower Rutbah	Rutbah 4	7	77	38	-	2m
	Rutbah 3	14	99	54	27	-
	Rutbah 2	1	109	36	18	-
	Rutbah 1	3	64	20	-	2m
Mulussa F. Clastic	Mul. cl3	0	100	31	-	2m
	Mul. cl2	0	91	28	14	-
	Mul. cl1	0	292	112	-	2m

Table 4.5: Definition of the layering in 2013 reservoir model

Then, the 5 electrofacies defined in the sedimentological model were quantified from core and log data, in order to be used in the simulation of the properties. Figure 4.19 and Table 4.6 illustrate the quantification of the electrofacies properties. These values were used for the rock type simulation on the grid.

		PHIE				SWE				SGR				VSH			
	LOGS	min	max	average	std. Dev	min	max	average	std. Dev	min	max	average	std. Dev	min	max	average	std. Dev
	EZT 401	0.08	0.21	0.15	0.03	0.01	1.00	0.47	0.37	6.62	31.42	12.99	6.00	0.01	1.00	0.47	0.38
	EZT 402	0.03	0.21	0.16	0.03	0.01	1.00	0.34	0.36	10.00	49.22	14.06	6.90	0.00	1.00	0.34	0.36
	EZT 403	0.00	0.26	0.14	0.03	0.01	1.00	0.37	0.33	15.01	34.99	23.15	5.74	0.00	1.00	0.35	0.34
	EZT 404	0.00	0.23	0.11	0.04	0.00	1.00	0.49	0.33	35.02	104.89	51.99	17.69	0.00	1.00	0.48	0.33
	EZT 405	0.00	0.22	0.06	0.39	0.00	1.00	0.66	0.36	50.03	271.38	90.53	32.04	0.00	1.00	0.62	0.37

		Phi plug H				Kg plug H				LOG10(Kg_H)				Equation	
	CORE	min	max	average	std. Dev	min	max	average	std. Dev	min	max	average	std. Dev	a	b
	401	4.53	22.51	17.39	3.03	7.70	2364.71	1160.95	717.86	0.89	3.37	2.90	0.50	0.10	1.19
	402	9.78	21.90	16.43	2.85	1.15	2953.59	851.16	674.43	0.06	3.47	2.62	0.71	0.16	-0.06
	403	2.45	20.57	14.87	3.34	0.10	2143.70	584.66	580.18	-1.00	3.33	2.17	1.20	0.22	-1.13
	404	1.99	22.20	12.45	4.94	0.00	2141.50	209.36	431.14	-3.00	3.33	0.40	1.97	0.33	-3.69
	405	0.63	21.36	7.80	5.07	0.00	1494.82	59.26	253.94	-3.00	3.17	-0.60	1.30	0.18	-1.99

Table 4.6: Result of the quantification of electrofacies from logs (upper table) and from core (lower table)

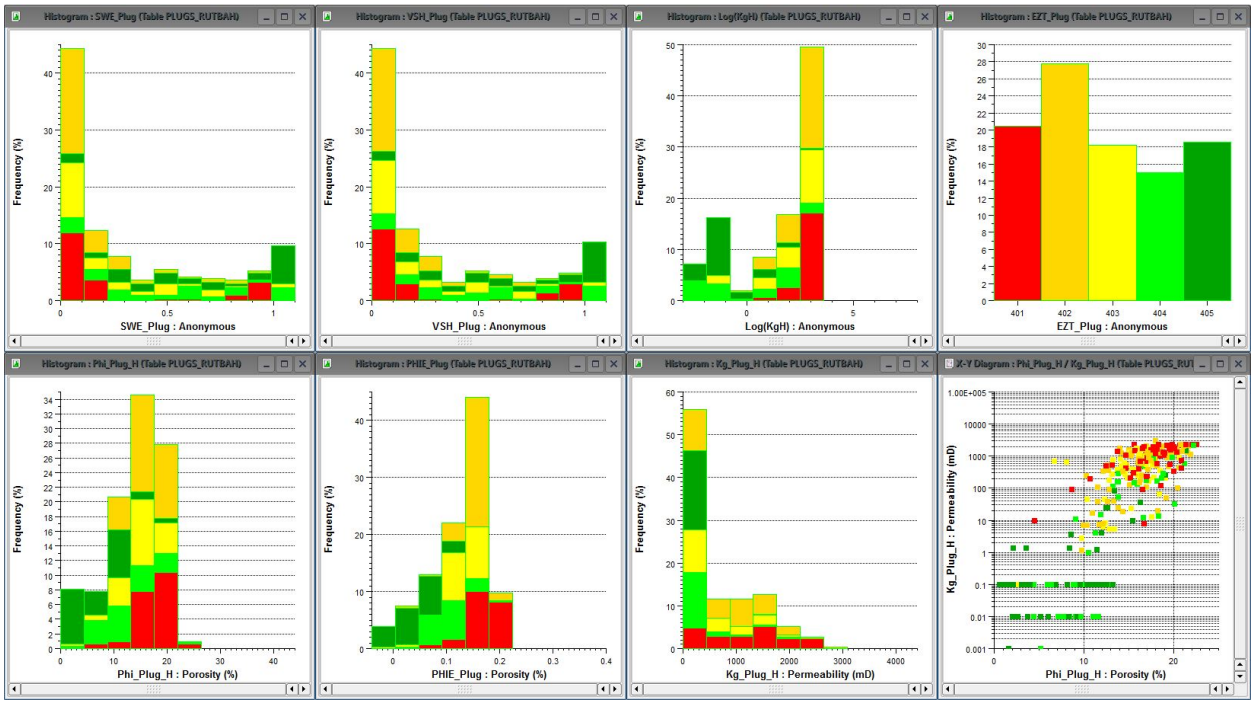

Figure 4.19: Histograms showing the distribution of properties for each electrofacies.

Afterwards, the simulation of facies and petrophysical properties (permeability, porosity and Net/Gross) was performed using specific variograms computed for each zone.

Two types of approaches were applied to the reservoir to fill the grid with properties. In Figure 4.20.shows the parameters using in each case. For the Lower Rutbah Fm, a pixel-based approach was used (Figure 4.21). This approach uses geostatistical techniques for the simulation of properties in each cell of the reservoir grid (cell=pixel).

The properties of the Mulussa clastic Fm were simulated using an object-based approach, in which the sand bodies are geometrically defined and distributed on the grid (Figure 4.22).

U. Rutbah : pixel-based approach

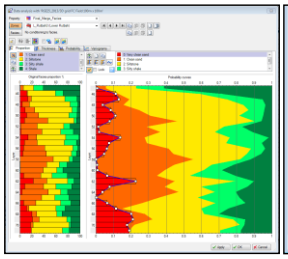

vertical proportion curve

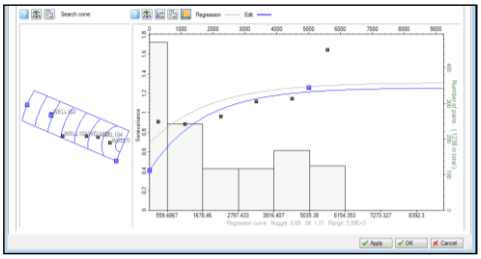

variograms

Mul. Clast : object based approach

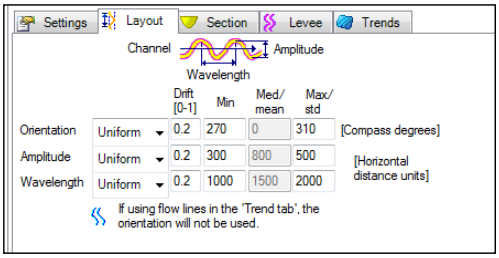

definition of the object geometry

Figure 4.20: Parameters used in both pixel and object-based approaches

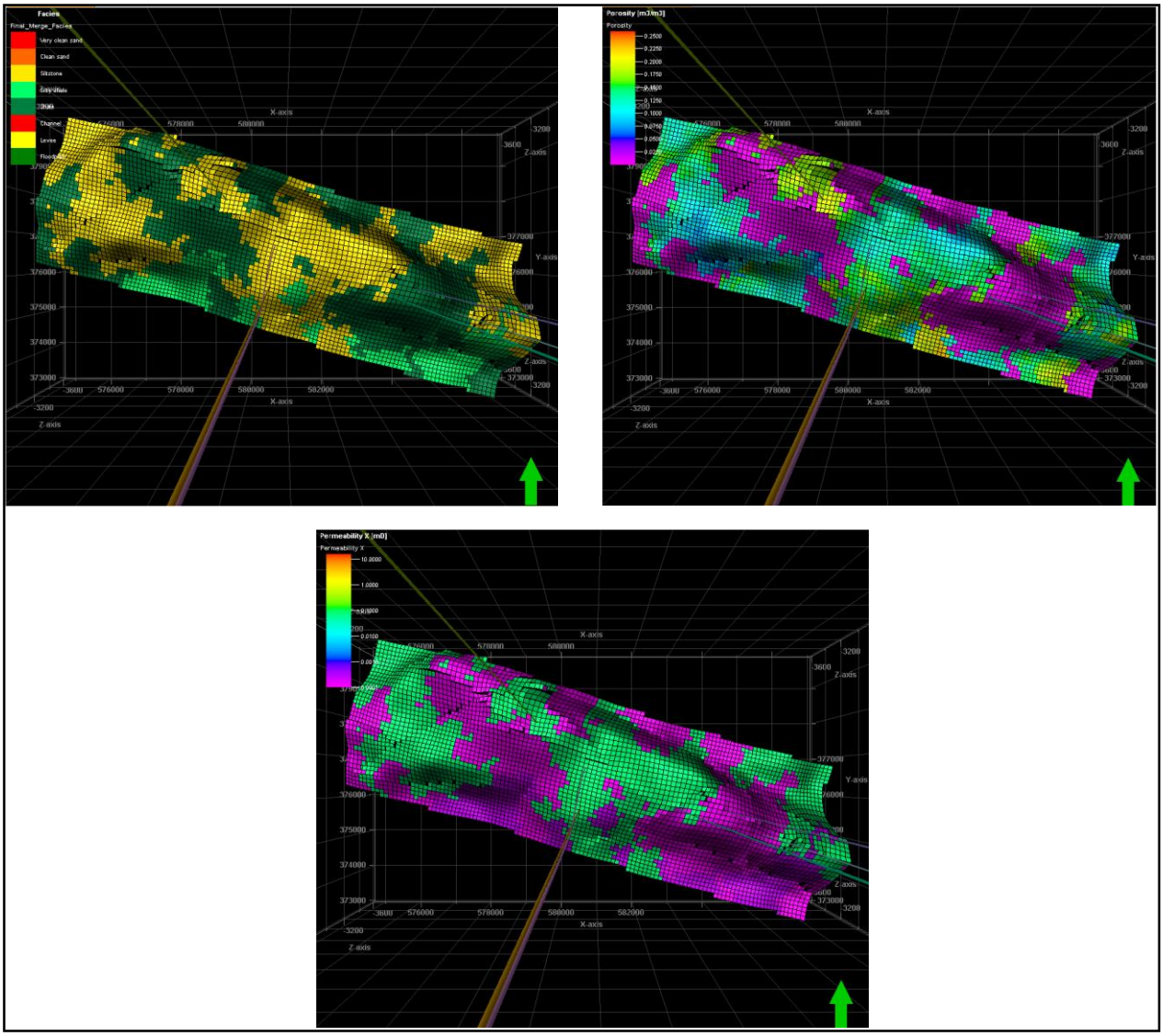

Figure 4.21: Top view of the facies, porosity and permeability properties simulated in the Lower Rutbah using a pixel-based approach.

In the Lower Rutbah Fm, individual sand-bodies such as channels or mouth bars cannot be recognized after simulation as the pixel-based modeling is only constrained by wells, with a minimum spacing of 1 Km. However the main facies trends observed on the correlation panel can be followed on the grid. The distribution of the main heterogeneities are preserved in the simulation.

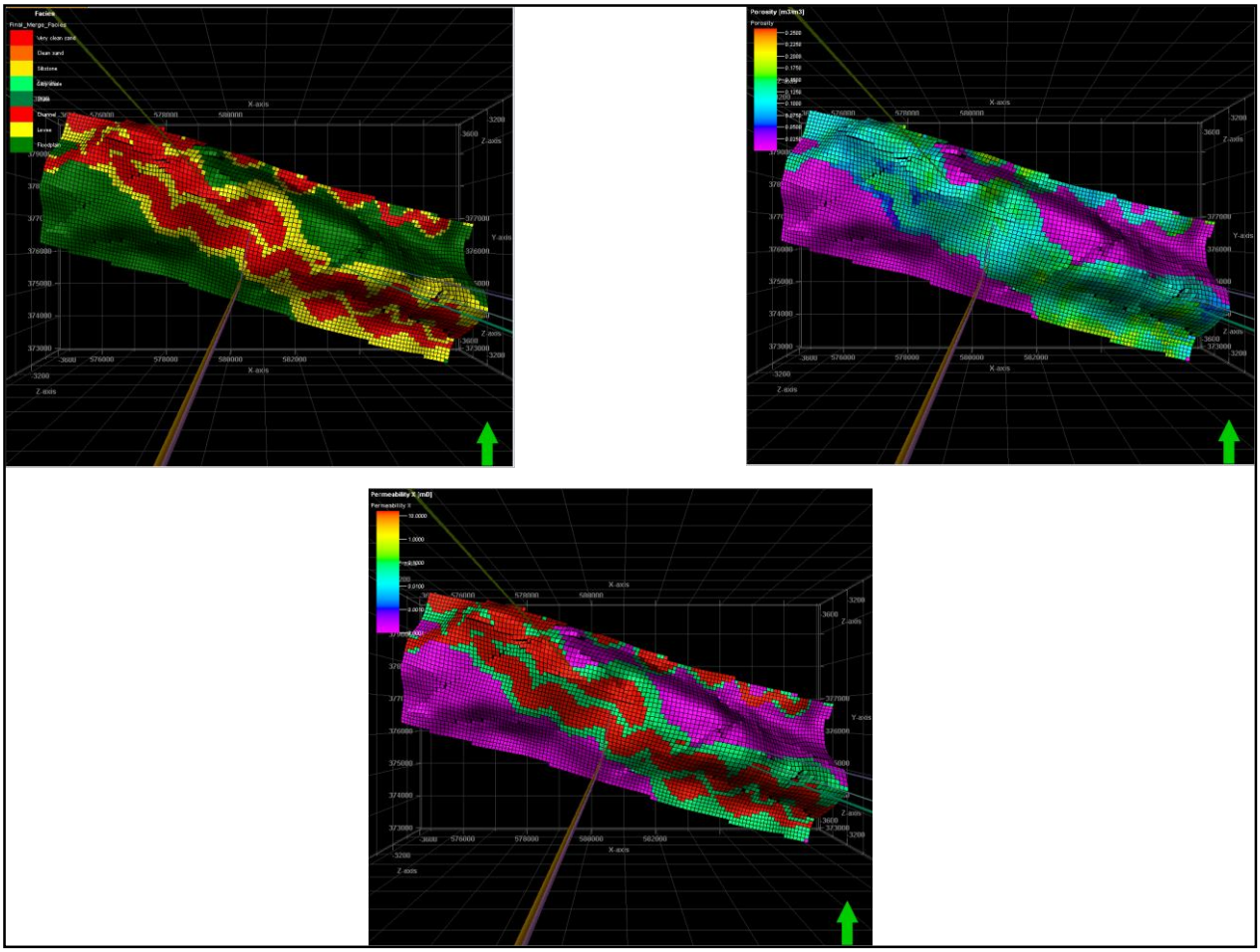

Figure 4.22: Top view of the facies, porosity and permeability properties simulated in the Mulussa cl Fm using an object-based approach.

In the Mulussa F clastic Fm, simulated with an object-based approach, it is possible to recognize channels with low sinuosity, as configured in the geometrical settings. The porosity decreases from the channel to the levee with the lowest values for the floodplain.

5. DISCUSSION

In this chapter, I will present the discussion of the new results obtained in the structural model, the sedimentalogical model and the stratigraphic model, and how these new inputs improved the static geological model of the FC field.

In addition, a discussion of the main uncertainties in the model is presented. In the chapter of conclusion will be discussion the improvements that could be useful in future models for the FC field and for other fields (affected by complex structural setting) in order to avoid the principal uncertainties and also to be used as a case study for academic purposes are given.

Structural model

Interpretation of the fault system

In the interpretation of the faults at least three fault trends were identified, where the NW-SE fault trend crosses the NE-SW fault trend. The chronology of these events could have implications for the preservation of the hydrocarbons in the area.

These faults trends seem to have a conjugate system relationship, produced during the same deformation event in the Late Cretaceous, indicating sinistral strike slip around the NW-SE direction. (Litak et al. 2001). In this case, the integrity of the trap could not be affected.

On the other hand, this fault framework could be related to fault reactivation on normal growth faults, in which the pre-existing discontinuity orientation affected the evolution of the main faults orientation and the secondary faulting associated with the main faults (Bellahsen 2005).
This could be another scenario for this configuration because a rifting in the Euphrates Graben began during the Late Cretaceous but became more active during

the Campanian and the Early Maastrichtian. Litak (1998) suggested a reorientation of the stress direction and a slowing of the extension of the rifting in the Early Maastrichtian. For this reason these changes in the faults direction could be interpreted as a reactivation of the previous fault system. In this case, the integrity of the traps created during the Late Cretaceous could be affected. In this model, it is not possible to define which of the processes was involved.

Interpretation of thickness variations

Paleogeography and subsidence during the Upper Triassic in the area of study had a strong influence on the spatial distribution of the Mulussa F clastic Formation. Considering a constant thickness in this formation was then not appropriate in the 2011 model and did not give a realistic scenario for the geological model. In addition, the same hypothesis was made for the Upper Rutbah Fm. in 2011.

As a result, in the 2013 model the picking of the Upper Rutbah and Mulussa F dolomite Formation on the seismic cube allowed for a more realistic thickness of the reservoirs and permitted us to define the spatial variations during the age of the deposition of these two units.

The main variation of the thickness for both units was recognized in the southwesten part of the area. This could imply a depocenter in this part. However, the paleogeographic context during these times locates the main source area to the southeast. It seems to be related more to subsidence at the same time as the deposition rather than with the paleogeographic configuration.

Interpretation of unconformities

The resolution of the seismic cube is low and the picking of the unconformity contact between Lower Rutbah Fm. and Mulussa F clastic was not possible.
As this unconformity is related to the uplift and erosion stage during the Jurassic, we expected to observe features in the seismic cube such as onlaps and toplaps in

this interval due to the unconformity. Moreover, the seismic characteristics of the two formations do not allow us to recognize the contact because of the low contrast of acoustic impedance between the Upper Triassic and Lower Cretaceous sandstones.

For this reason, I was not able to interpret the Top Lower Rutbah and the Top Mulussa F clastic and I had to interpolate them from the Top Upper Rutbah and Top Mulussa F dolomitic and then calibrate them with the well tops. These processes introduce uncertainties into the model, and could alter the volumetric calculations in the model.

Faults and field compartmentalization

The 2013 model used 4 faults interpreted in the previous model. These 4 faults are necessary in order to create the compartmentalization of the wells 102, 103 and 104. However, these faults were not recognized on the seismic cube. As a result, the exact location of those faults are unreliable in the 2013 model.

Model boundary

All the faults in the seismic cube were picked in the 2013 model. It could be helpful to change the limits of the model and extend it in order to determine if there are prospective areas. However, in this case the complexity of the model could be increased and thus become useless as a case study for academic purposes.

Velocity model

The depth-time conversion on the project only used the well tops and the values of the interval velocity calculated from the check shot 103. In the velocity model the values from the VRMS cube were not taken into account in order to achieve better results during the conversion. Improvements in the velocity model could be necessary for future models.

Sedimentological model

In the sedimentological model, I defined the paleogeographic setting for the Rutbah and Mulussa F Fm based on literature. For both formations, the coastline was located to the northwest and the source area of the system was located to the southeast. The Mulussa F Fm was linked to the Hamad Uplift while the Rutbah was related to the Rutbah high.

In this context, I expected coarser-grained material close to the uplift. However, for the Lower Rutbah Formation I found coarser-grained sandstone in well 102 than in the other wells, and it was supposed to be further from the source area. Thus, I considered that this anomalous content could be related to small paleo-depocenters in the area instead of associated with a change of the paleogeographic configuration.

On the other hand, for the Mulussa F clastic I recognized the highest thickness in well 103 which is located around the same distance from the source area; however, the thickness is almost double. It could be related to a local subsidence during the Upper Triassic that drained the fluvial system. For this reason, I tried to determine this configuration and also the elongation and continuity of the channels using attributes on the seismic cube such as coherence cube, extraction of amplitudes, but the quality of the seismic cube did not allow for accurate results.

It is important to note that the paleogegraphic configuration is not clear for these times in the area. Given the limited available information it was impossible to define a specific paleogeography for the case study vicinity and we had to use the information coming from the regional setting.

Stratigraphical model

The correlation of the MFS permitted the model to preserve the main heterogenities in the system, because a MFS corresponds to a regional event in the geological record. I used these time lines to correlate and subsequently define the zones in the

static geological model. However, the inter-well distance is around 1 to 2 kilometers and, in this interval we can expect lateral variations that are impossible to capture without more data (new wells, new seismic). Thus, some uncertainties are introduced into the model regarding the continuity of the reservoir properties.

In addition, the correlation of the sand-bodies was performed by taking into account the information of the relationship between the thickness and width given for the channels of the Mulussa F clastic Fm. With the limited information about paleogeography, I could not refine neither the reconstruction of the system, nor the elongation of the sand-bodies.

In the database of the Lower Rutbah Formation core, there is a description of a cementing event of a few tens of centimeters in the very fine-grained sandstones and siltstone associated with distal mouth bar and coastal plain environments. But I could not determine how the properties of the reservoir could be affected by these cemented layers neither if there were common features in the others wells. These layers could create heterogeneities in the field. However, in the 2013 model this heterogeneities could not be modeled. More information and characterization of this specific heterogeneity is requested for a better prediction of the reservoir properties.

Geological static model

The 2013 model was more focused on the geological aspects than on the reservoir aspects and this is the main improvement. As a result, the structural model, the sedimentological model and the stratigraphic model were created as an input for the static model. Meanwhile, the 2011 model was more dedicated to reservoir purposes, which was the main objective for the Field Challenge competition.

The FC field presents compartmentalized blocks, which were possible to define using pressure data from the wells. The 2011 model used 21 faults and the 2013 model used 20 faults, in order to preserve the compartmentalization of the field. Thus, it was not possible to simplify the 2011 model in this aspect.

In the 2011 model, 4 zones were created for the Lower Rutbah and 5 for the Mulussa F clastic; these 9 zones were considered as flow units. In the 2013 model 7 zones were created in total: 4 in the Lower Rutbah and 3 in the Mulussa F clastic . This reduction of zones could simplify the 2013 model. However, I increased the number of layers in order to preserve a greater heterogeneity level than in the 2011 model. Thus, it is difficult to simplify the 2013 model without dynamic data to evaluate the dynamic behavior of the new model.

Dynamic data

The areal extension of the 2011 model is bigger than in the 2013 model, with an irregular boundary which could create problems in the direction of the gridding and subsequently in the fluid flow simulation. For this reason a rectangular boundary was used in the 2013 model, with the long axis in the direction of flow to reduce numerical problems and optimize the flow simulation (Figure 5.1).

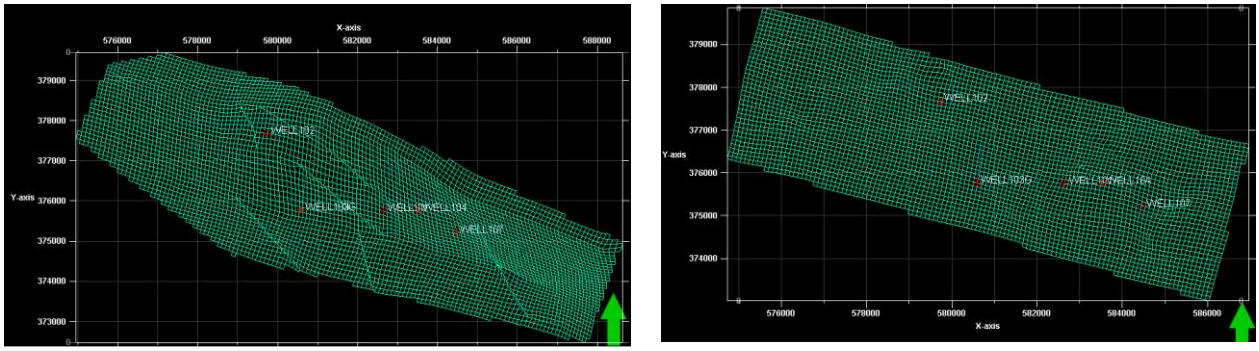

Figure 5.1: Comparison between the boundaries of the 2011 model (left) and the 2013 model (right)

In the 2013 study, the time-depth conversion was performed before gridding, while the 2011 model was built in the time domain and converted to depth afterwards. The best way to perform a static model is still in debate - either in the depth domain or in the time domain. So it is difficult to define the impact this choice will have on the results.

In addition, in the 2013 model the faults were modeled as zig-zag type faults instead of linear type faults, as modeled in the 2011 model. I cannot determine if this parameter simplifies or complexities the model without the inclusion of dynamic data.

6. CONCLUSIONS

The 2013 model of the FC field was created with the inclusion of a new structural model, a new sedimentological model, and a new stratigraphical model using the same database as the 2011 model.

The 2013 model is considered a more realistic geological case than 2011 model, because the complete interpretation of the database gave us more confidence in the following aspects:

- Thickness of the reservoirs (Lower Rutbah and Mulussa F clastic).
- Structural framework.
- Environment of deposition based on core data (Deltaic system and Fluvial system).
- Definition of the stratigraphic/reservoir units based on the correlation of the main Maximum Flooding Surfaces (MFS).
- Definition of 5 electrofacies based on SGR log data for the Lower Rutbah and Mulussa F clastic.
- Simulation of the property distribution in the Rutbah with a pixel-based approach and in the Mulussa F clastic with an object-based approach.

The main heterogeneities identified correspond to increasing shaliness in the reservoir due to the environment of deposition and fluctuations in the relative sea level. For this reason 7 zones were defined as stratigraphic units in the model; 4 zones within the Lower Rutbah and 3 zones within the Mulussa F clastic. These zones can be defined by the relationship between shaliness and MFS through geological time.

The compartmentalization in the FC field is due to the normal faulting that occured during the Upper Cretaceous. However, the lithostratigraphic sequences may also produce compartmentalization on a lower scale than the faults.

The simplification of the 2013 model consist in:

- Reduction of the aerial size of the model and the grid direction (NW-SE) which is correlated with the main fault trend.
- Reduction of zones from 9 in the 2011 model to 7 in 2013 model.
- Some parameters for the geostatistical simulation are common to several zones.

The main uncertainties were identified in:

- Interpretation of the main horizons due to the low resolution of the seismic information.
- Depth-time conversion due to the only VSP information in one well over an area of 180km^2.
- Variation in the thickness and in the areal extension of the reservoir.

7 FUTURE IMPROVEMENTS

In the FC field a new interpretation of the main horizons, the log and the core, along with new parameters in the static geological model allowed us to build a more realistic model with more confidence in the results obtained. In addition, there is also a clear workflow to be used in a case study for academic purposes, taking into account the limited duration of a course.

Improvements in the velocity model could give an accurate depth-time conversion far from well 103, which is the only one with VSP data. In addition, inclusion of more data in the model, such as new cores from the new wells that have been drilled in the field during the last few years could reduce the uncertainties in the stratigraphical model as well as in the sedimentological model.

The seismic cube presents a low quality resolution for stratigraphical aspects, and new seismic data have been acquired on the area. The interpretation of that data and the use of the attributes could reduce the uncertainties in the surfaces that I cannot pick as well as on the extension of the faults and the elongation and direction of the sand-bodies.

If the new seismic cube was not available, a new seismic inversion of the first cube could bring more information for the picking and the interpretation. A feasibility study could then be launched on this new inversion data to evaluate if any information could be extracted to better constrain the static reservoir model: map of porosity, probability of sand, ...

It is important to upscale the 2013 model and introduce dynamic data in order to recognize if the model matches with the historical data and if certain improvements are required.

8. BIBLIOGRAPHY

Bellahsen, N. and J.M. Daniel 2003. Fault reactivation control on normal fault growth: an experimental study. Journal of Structural Geology, no. 27, p. 769-780.

Best, J.A., 1991. Crustal evolution of the northern Arabian platform beneath the Syrian Arab Republic. Unpublished PhD thesis, Cornell University, Ithaca, New York. 152 p.

Best, J.A., M. Barazangi, D. Al-Saad, T. Sawaf and A. Gebran 1993. Continental margin evolution of the northern Arabian platform in Syria. American Association of Petroleum Geologists Bulletin, v. 77, no. 2, p. 173–193.

Beydoun, Z.R. 1991. Arabian plate hydrocarbon geology and potential—a plate tectonic approach., American Association of Petroleum Geologists, Studies in Geology, 33, 77 p.

Brew, G., M. Barazangi, K. Al-Maleh and T. Sawaf 2001. Tectonic and Geologic Evolution of Syria. GeoArabia, Vol. 6, No. 4.

Brew, G.E., R.K. Litak, D. Seber, M. Barazangi, A. Al-Imam and T. Sawaf 1997. Basement depth and sedimentary velocity structure in the northern Arabian platform, eastern Syria. Geophysical Journal International, v. 128, no. 3, p. 617–631.

Brew, G., R. Litak, M. Barazangi and T. Sawaf 1999. Tectonic evolution of northeast Syria: regional implications and hydrocarbon prospects. GeoArabia, v. 4, no. 3, p. 289–318.

Chaimov, T., M. Barazangi, D. Al-Saad, T. Sawaf and A. Gebran 1992. Mesozoic and Cenozoic deformation inferred from seismic stratigraphy in the southwestern intracontinental Palmyride fold-thrust belt, Syria. Geological Society of America Bulletin, v. 104, no. 6, p. 704 715.

Cohen, Z., V. Kaptsan and A. Flexer 1990. The tectonic mosaic of the southern Levant: implications for hydrocarbon prospects. Journal of Petroleum Geology, v. 13, no. 4, p. 437 462.

Collinson, J.D. Alluvial sediments. In: Department of Earth Sciences, University of Oxford. Sedimentary Environments: Processes, Facies and Stratigraphy. 1996. p. 37-82.

Ruiter, R.S.C., P.E.R. Lovelock and N. Nabulsi 1994. The Euphrates Graben, Eastern Syria: a new petroleum province in the northern Middle East. In, M.I. Al-Husseini (Ed.), Middle East Petroleum Geosciences, GEO'94. Gulf PetroLink, Bahrain, v. 1, p. 357–368.

Gvirtzman, G. and T. Weissbrod 1984. The Hercynian geanticline of Helez and the late Palaeozoic history of the Levant. In, J.E. Dixon and A.H.F. Robertson (Eds), Geological Society, London, Special Publication no. 17, p. 177–186.

Haq, B.U., J. Hardenbol and P.R. Vail 1988. Mesozoic and Cenozoic chronostratigraphy and cycles of sea-level change. In C.K. Wilgus, B.S. Hastings, C.A. Rosset al (Eds.), Sea-level changes; an integrated approach. Society of Economic Paleontologists and Mineralogists, Special Publication 42, p. 72–108.

Hempton, M. 1985. Structure and deformation of the Bitlis suture near Lake Hazar, southeastern Turkey. Geological Society of America Bulletin, v. 96, no. 2, p. 233–243.

Husseini, M.I. 1989. Tectonic and deposition model of late Precambrian-Cambrian Arabian and adjoining plates. American Association of Petroleum Geologists Bulletin, v. 73, no. 9, p. 1117–1131.

Husseini, M.I. 1992. Upper Palaeozoic tectono-sedimentary evolution of the Arabian and adjoining plates. Journal of the Geological Society, London, v. 149, no. 5, p. 419–429.

Jamal.
., M., Y. Bizra and C. Caron 2000. Palaeogeography and hydrocarbon hábitat of the Triassic series in Syria. Earth and Planetary Sciences, no. 331, p. 133-139.

Johnson, H.D. and C.T. Baldwin. Shallow clastic seas. In: Department of Earth Sciences, University of Oxford. Sedimentary Environments: Processes, Facies and Stratigraphy. 1996. p. 232-280.

Kohn, B., M. Eyal and S. Feinstein 1992. A major Late Devonian-Early Carboniferous (Hercynian) thermotectonic event at the NW Margin of the Arabian-Nubian Shield: evidence from zircon fission track dating. Tectonics, v. 11, no. 5, p. 1018–1027.

Laws, E.D. and M. Wilson 1997. Tectonics and magmatism associated with the Mesozoic passive continental margin development in the Middle East. Journal of the Geological Society, London, v. 154, no. 3, p. 459–464.

Litak, R.K., M. Barazangi, G. Brew, T. Sawaf, A. Al-Imam and W. Al-Youssef 1998. Structure and Evolution of the Petroliferous Euphrates Graben System, Southeast Syria. AAPG Bulletin, v. 82, no. 6, p. 1173-1190.

Litak, R.K., Barazangi, M.; Beauchamp, W.; Seber, D.; Brew, G.; Sawaf, T. and Al-Yousef, W. (1997): Mesozoic-Cenozoic evolution of the intraplate Euphrates Fault System, Syria: Implications for regional tectonics. Journal of the Geological Society, London, 154 (4), p. 653-666.

Lovelock, P.E.R. 1984. A review of the tectonics of the northern Middle East region. Geological Magazine, v. 121, no. 6, p. 577–587.

Makaske B., 2001. Anastomosing rivers: a review of their classification, origin and sedimentary products. Earth-Science Reviews 53. p 149-196

Mouty, M. 2000. The Jurassic in Syria: an overview. Lithostratigraphic and biostratigraphic correlations with adjacent areas. In, S. Crasquin-Soleau and E. Barrier (Eds.), New data on PeriTethyan sedimentary basins. Memoires du Muséum National d'Historie Naturelle, Paris, PeriTethys Memoir 5, p. 159–168.

Mouty, M. and Al-Maleh, K., 1983. The geological study of the Palmyridian chain using ideal geological sections for exploration purposes and geological survey. General Establishment of Geology and Mineral Resources, Syrian Ministry of Petroleum and Mineral Resources, Damascus, Syria, 'Unigeoconsult', no. 140, 4 volumes, 950 p.

Mouty, M., M. Delaloye, D. Fontignie, O. Piskin and J.-J. Wagner 1992. The volcanic activity in Syria and Lebanon between Jurassic and Actual. Schweizerische Mineralogische und Petrographische Mitteilungen, v. 72, no. 1, p. 91–105.

Olewczyńska, M., SPE, J. Grötsch, J. Al-Jundi and S. Rao 2005. High-Resolution Static/Dynamic Modelling and 3-Phase Streamline Simulation in Complex Fluviatile Reservoirs. International Petroleum Conference, IPTC 10896.

Ponikarov, V.P. 1966. The geology of Syria. Explanatory Notes on the Geological Map of Syria, scale 1:200 000. Ministry of Industry, Syrian Arab Republic.

Reading, H.G. and J.D. Collinson. Clastic coasts. In: Department of Earth Sciences, University of Oxford. Sedimentary Environments: Processes, Facies and Stratigraphy. 1996. p. 154-231.

Robertson, A.H.F. and J.E. Dixon 1984. Aspects of the geological evolution of the Eastern Mediterranean. In, J.E. Dixon and A.H.F. Robertson (Eds.), The Geologic Evolution of the Eastern Mediterranean. Geological Society, London, Special Publication no. 17, p. 1–74.

Sawaf, T., G.E. Brew, R.K. Litak and M. Barazangi 2001. Geologic evolution of the intraplate Palmyride Basin and Euphrates fault system, Syria. In, W. Cavazza, A. Robertson and P. Ziegler (Eds.), PeriTethyan rift/wrench basins and passive margins, Memoires du Muséum National d'Historie Naturelle, Paris, PeriTethys Memoir 6.

Sharland, P.R., R. Archer, D.M. Casey, R.B. Davies, S.H. Hall, A.P. Heward, A.D. Horbury and M.D. Simmons 2001. Arabian Plate sequence stratigraphy. GeoArabia Special Publication 2. Gulf PetroLink, Bahrain, 371 p.

Sharland, P.R., R. Archer, D.M. Casey, R.B. Davies, S.H. Hall, A.P. Heward, A.D. Horbury and M.D. Simmons 2001. Arabian Plate sequence stratigraphy. GeoArabia Special Publication 2. Gulf PetroLink, Bahrain, 371 p.

Stampfli, G.M., J. Mosar, P. Favre, A. Pillevuit and J.-C. Vannay 2001. Permian-Triassic evolution of the western Tethyan realm: the NeoTethys/east Mediterranean basin connection. In, W. Cavazza, A.H.F. Robertson and P. Ziegler (Eds.), PeriTethyan rift/wrench basins and passive margins. Memoires du Muséum National d'Historie Naturelle, Paris, PeriTethys Memoir 6.

Stoeser, D.B. and V.E. Camp 1985. Pan-African microplate accretion of the Arabian shield. Geological Society of America Bulletin, v. 96, no. 7, p. 817–826.

Walley, C. 2001. The Lebanon passive margin and the evolution of the Levantine Neotethys. In, W. Cavazza, A.H.F. Robertson and P. Ziegler (Eds.), PeriTethyan rift/wrench basins and margins. Memoires du Muséum National d'Historie Naturelle, Paris, PeriTethys Memoir 6.